**Biogeosciences
Discussions**

Biogeosciences Discussions is the access reviewed discussion forum of *Biogeosciences*

BGD

6, 5163–5215, 2009

**A dynamic climate
state during the
Paleocene-Eocene
Thermal Maximum**

A. Sluijs and H. Brinkhuis

A dynamic climate and ecosystem state during the Paleocene-Eocene Thermal Maximum – inferences from dinoflagellate cyst assemblages at the New Jersey Shelf[*]

A. Sluijs and H. Brinkhuis

Palaeoecology, Institute of Environmental Biology, Utrecht University, Laboratory of Palaeobotany and Palynology, Budapestlaan 4, 3584 CD Utrecht, The Netherlands

Correspondence to: A. Sluijs (a.sluijs@uu.nl)

[*]Invited contribution by A. Sluijs, one of the EGU Outstanding Young Scientist Award winners 2007.

Abstract

Late Paleocene and Early Eocene climates and ecosystems underwent significant change during several transient global warming phases, associated with rapidly increasing atmospheric carbon concentrations, of which the Paleocene-Eocene Thermal Maximum (PETM; ~55.5 Ma) is best studied. While biotic response to the PETM as a whole (~170 kyrs) has been relatively well documented, variations during the PETM have been neglected. Here we present organic dinoflagellate cyst (dinocyst) distribution patterns across two stratigraphically expanded PETM sections from the New Jersey Shelf, "Bass River" and "Wilson Lake". Many previously studied sites show a uniform abundance of the thermophilous and presumably heterotrophic taxon *Apectodinium* that spans the entire carbon isotope excursion (CIE) of the PETM. In contrast, the New Jersey sections show large variations in abundances of many taxa during the PETM, including the new species *Florentinia reichartii* that we formally propose. We infer paleoecological preferences of taxa that show temporal abundance peaks, both qualitative and absolute quantitative, from empirical as well as statistical information, i.e., principle (PCA) and canonical correspondence analyses (CCA). In the CCAs, we combine the dinocyst data with previously published environmental proxy data from these locations, such as TEX_{86} paleothermometry, magnetic susceptibility and sedimentary size fraction. The combined information supports previous inferences that sea level rose during the PETM, but also indicates a (regional) increase in fresh-water runoff that started ~10 kyr after the onset of the CIE and perhaps precession-paced cycles in sea surface productivity. The highly variable dinocyst assemblages of the PETM contrast rather stable Upper Paleocene assemblages, which suggests that carbon input caused a dynamic climate state, at least regionally.

A. Sluijs and H. Brinkhuis

1 Introduction

Now that almost everyone expects a certain amount of global warming by the end of the century, interest to climate change as a whole is increasing. Global and regional climate models expect an increase in year-to-year variability of weather resulting from increasing CO_2 concentrations (e.g., Diffenbaugh et al., 2008). If so, one may expect increasing variability in climate over the coming centuries, millennia and even longer time scales, because carbon concentrations in the atmosphere are expected to remain high for several hundreds of thousands of years (Archer, 2005). One way to assess climate dynamics in a rapidly warming world is to perform high-resolution paleoenvironmental reconstructions on high-accumulation rate sediment sections deposited during a past analogue, such as the Paleocene-Eocene Thermal Maximum (PETM).

The PETM represents a ∼170 kyr (Röhl et al., 2007; Abdul Aziz et al., 2008) lasting episode of extreme global greenhouse warmth ∼55.5 Million years ago (Ma), superimposed on the already warm Late Paleocene and Early Eocene (Bowen et al., 2006; Sluijs et al., 2007a). The onset of the PETM marks an additional warming of ∼5–9°C Kennett and Stott, 1991; Sluijs et al., 2006) and a pronounced negative stable carbon isotope ($\delta^{13}C$) excursion (CIE), measured in marine and terrestrial sedimentary components (Kennett and Stott, 1991; Koch et al., 1992; Schouten et al., 2007). The CIE is widely taken to evidence the injection of large amounts of ^{13}C-depleted carbon in the shape of CH_4 and/or CO_2 into the ocean-atmosphere system (Dickens et al., 1995, 1997). This addition of "light" carbon is generally thought to lie at the root of this episode of extreme global warmth (Higgins and Schrag, 2006; Pagani et al., 2006), or to represent a positive feedback to warming, for example through the melting of submarine methane hydrates (Dickens et al., 1995; Sluijs et al., 2007b).

Although warming and perturbations in the hydrological cycle during the PETM as a whole is relatively well documented, not much is known about climate changes during the PETM. Generally, biotic and geochemical records suggest a relatively uniform, warm climate state over the span of the PETM. At least partially, this is due to many

A. Sluijs and H. Brinkhuis

Printer-friendly Version

Interactive Discussion

studies using extremely condensed deep-sea sediment sections, where bioturbation has potentially blurred signals and carbonate dissolution reduced temporal resolution, particularly for the onset of the event (Zachos et al., 2005). Expanded sections show much more detail; for example, continental sections comprised of stacked paleosols such as those in the Bighorn Basin, Wyoming, USA, have high accumulation rates and have revealed wet and dry phases (Bowen et al., 2004; Wing et al., 2005; Kraus and Riggins, 2007), as well as precession-forced variations in hydrology (Abdul Aziz et al., 2008) within the PETM.

In the marine realm, particularly oil exploration and production companies have re-trieved many high accumulation PETM sections from the continental shelves. From the comparatively few marginal marine sections from which biogeological data are publically available it has become clear that among morphologically recognizable re-mains of eukaryotic planktonic biota, the dinoflagellates exhibit the most dramatic re-sponse across the PETM (Sluijs et al., 2007a). This notably through the quasi-globally recorded acme of the organic cysts (or dinocysts) of the thermophilous, and possibly heterotrophic taxon *Apectodinium* (Bujak and Brinkhuis, 1998; Crouch et al., 2001, 2003a; Egger et al., 2003). Recent studies have focussed on high-accumulation rate, expanded marginal marine PETM cores from New Jersey, USA, named "Wilson Lake" (Gibbs et al., 2006; Zachos et al., 2006) and "Bass River" (Cramer et al., 1999), drilled by the United States Geological Survey (USGS) and the Ocean Drilling Program (ODP), respectively (Fig. 1). These studies showed that the onset of the *Apectodinium* acme represents the earliest sign of anomalous PETM-related environmental change, as it occurred several kyrs prior to the onset of warming and the subsequent initiation of the CIE (Sluijs et al., 2007b).

Since sediment accumulation rates were ∼10 cm/kyr across the PETM on the New Jersey Shelf, on average, these sections are potentially well suited to assess infra-PETM climate dynamics. Here we attempt to contribute by paleoecological evaluation of the PETM dinocyst distribution patterns against the background of the combined multidisciplinary New Jersey paleoenvironmental datasets related to e.g., sea surface

A dynamic climate state during the Paleocene-Eocene Thermal Maximum

A. Sluijs and H. Brinkhuis

temperature (planktonic foraminifer δ^{18}O, TEX$_{86}$), energy level of the sedimentary environment (bulk sediment grain size), productivity (calcareous nannofossils) and river supply of terrigenous matter (Branched and Isoprenoid Tetraether (BIT) index, and clay flux data). With this approach, we aim to detect environmental trends within the PETM to eventually contribute to the understanding of processes underlying, and effects of rapid global warming and exogenic carbon release in a greenhouse world.

2 Material and methods

2.1 Material

The Bass River core (39°36′42″N, 74°26′12″W) was drilled in Bass River State Forest, New Jersey, during ODP Leg 174AX in 1996 (Miller et al., 1998). The Wilson Lake core (39°39′N, 75°03′W) was drilled by the USGS in 2000 and is located approximately 30 km west of Bass River, e.g., closer to the paleoshoreline. Previously published lithological and micropaleontological information indicated that the New Jersey sites were located on the shelf during the PETM (Gibson et al., 1993; Gibson et al., 2000). Uppermost Paleocene sediments of the Vincetown Formation at both sites are relatively condensed (average sedimentation rates of ~1 cm kyr^{-1}) and consist of glauconite-bearing siltstones, interpreted as a transgressive systems tract (Liu et al., 1997; Cramer et al., 1999) (Figs. 2, 3). The PETM was previously identified at both sites, based on the CIE in calcite and dinocyst δ^{13}C records (Cramer et al., 1999). Based on these records, the onset of the CIE is at 357.3 m below surface (mbs) at Bass River (Fig. 2). In the δ^{13}C record measured on bulk carbonate (BC) at Wilson Lake, the base of the CIE is not as clearly marked as at Bass River, primarily due to the absence of carbonate between ~109.3 and ~109.8 mbs (Fig. 3). The δ^{13}C record measured on dinocysts (DINO) shows background upper Palaeocene values up to ~110.0 mbs. At this level the transition to true CIE values starts, coinciding with a negative step in the δ^{13}C$_{BC}$ record, together implying the base of the CIE to be at this level (Sluijs et

al., 2007b). The onset of the CIEs marks the transition to the Manasquan formation, and the entire CIE is rich in clay, particularly kaolinite, and devoid of siliciclastic coarse fraction (Cramer et al., 1999). The CIEs comprise very expanded deposits that exhibit sedimentation rates of approximately 8–10 cm kyr^{-1} (Gibbs et al., 2006; Sluijs et al., 2007b; John et al., 2008). The upper part of the CIE is truncated in a sequence boundary at both sites, and sediments overlying this interval are at least 2 Myr younger than the PETM (Cramer et al., 1999).

2.2 Methods

2.2.1 Processing and analyses

Palynological processing was performed using standard methods described in, e.g., Sluijs et al. (2003). Briefly, ~10 g of freeze-dried sample, spiked with a known amount of *Lycopodium* spores, was treated with 30% HCl and twice with 38% HF for carbonate and silicate removal, respectively. Residues were sieved using a 15-μm nylon mesh, and subsequently mounted on microscope slides and analyzed under 500× magnification. All slides, incl. holotype materials, are lodged in the collection of the Laboratory of Palaeobotany and Palynology, Utrecht University, The Netherlands.

Dinoflagellate cyst ecology and grouping of taxa

It is generally assumed that most fossil organic (so-called "preservable") dinocysts represent the hypnozygotic stage of some species of dinoflagellates – less than 20% of species in the Modern for example (Fensome et al., 1996). Living organic cysts of dinoflagellates can be traced back to the motile stage (theca) through laboratory incubation experiments (e.g., Rochon et al., 2009). Increasingly, it is made clear that at least several modern dinoflagellate species may produce various cyst "morphotypes" depending on the chemophysical parameters of the water mass in which the theca develops or because of other, unknown ecological and/or biological, incl. genetic aspects

Title Page

Abstract | Introduction

Conclusions | References

Tables | Figures

◀ | ▶

◀ | ▶

Back | Close

Full Screen / Esc

Printer-friendly Version

Interactive Discussion

A dynamic climate state during the Paleocene-Eocene Thermal Maximum

A. Sluijs and H. Brinkhuis

(Ellegaard, 2000; Hallett, 1999). In the absence of fossilized genetic materials and/or relevant DNA/RNA studies, paleontologists have based dinocyst taxonomy on even the tiniest of morphological details, and differences in those details, observed in/on fossil remains. Unfortunately, seen in the light of the modern incubation experiments, it is notoriously difficult, if not impossible, to determine the true biological and/or ecological relevance of such details. Yet, in order to extract meaningful paleoecological information from fossil dinoflagellate remains, it is vital to establish whether recorded specimens represent relatively consistent biological or even ecological entities or not. Here, in order to at least assess some possible first order ecological relationships between apparently changing physiochemical parameters and dinocyst paleoecology we take an approach that is based on largely empirically based grouping of morphologically closely related forms. These taxa may either be strictly, or loosely defined accepted "species", groups of "species" within genera, genera themselves, or even groups of genera (cf. Brinkhuis, 1994; Pross and Brinkhuis, 2005; Sluijs et al., 2005). Next, we assume that any given high relative and/or high absolute abundance of these taxa per unit time reflects (sub)optimal environmental conditions and/or wider tolerance towards certain environmental conditions for such taxa. For example, a monotypic assemblage is taken to indicate that only that specific taxon was able to cope with apparently restricted marine, or even fresh water conditions.

For practical purposes, we follow the nomenclature cited in Fensome and Williams (2004). In the taxonomical section, we present the rationale for the established "eco" taxa employed herein.

Statistical analyses

For the principle component (PCA) and canonical correspondence analyses (CCA) we use the software package Canoco (ter Braak and Smilauer, 2002). In the CCAs we compare the dinocyst assemblages with TEX_{86}-derived sea surface temperatures (Sluijs et al., 2007b; Zachos et al., 2006), weight % sand (>63 μm sediment fraction) (John et al., 2008), BIT index (Sluijs et al., 2008a) and magnetic susceptibility.

3   Results

3.1   Dinocyst distribution patterns

Dinocyst assemblages are very similar in both relative and absolute abundances between Bass River and Wilson Lake, and generally comprise of taxa commonly recorded in mid-latitude marginal marine early Paleogene sediments (Figs. 2, 3). Upper Paleocene assemblages are either dominated by representatives of the typically open marine *Spiniferites* complex (cpx), or by members of the *Areoligera* cpx (Figs. 2, 3). Locally, we have recorded abundant representatives of the family Goniodomaceae, particularly *Eocladopyxis* spp., but also *Heteraulacacysta* spp. and *Polysphaeridium* spp., which are widely considered to be characteristic of restricted marine, usually lagoonal settings with generally high, but also (seasonally) variable salinities in the Modern (Reichart et al., 2004) and during the Paleogene (Brinkhuis, 1994). Just prior to the onset of the CIE, specimens assignable to *Apectodinium* spp. become dominant (Sluijs et al., 2007b). Particularly within the PETM, representatives of a suite of morphologically closely related Peridinioid genera are abundant (particularly those assignable to *Senegalinium* and *Phthanoperidinium*), a group that in general tolerated very low surface water salinities (Röhl et al., 2004; Brinkhuis et al., 2006; Sluijs et al., 2006, 2007b, 2008b), and likely preferred high nutrient and/or food supply (e.g., Dale and Fjellså, 1994; Sluijs et al., 2005). Additional locally common to abundant taxa include *Cordosphaeridium* spp., *Membranosphaera* spp., *Hystrichosphaeridium tubiferum*, *Operculodinium* spp., and one previously undescribed representative of *Florentinia*.

3.2   Site-to-site correlation

Prior to the PETM. both at Wilson Lake and Bass River assemblages are dominated by representatives of *Areoligera*, but diversity increases within the PETM. Because the sites are only ~30 km apart, changes in dinocyst assemblages on these timescales

should be concomitant between these sites if they represent regional rather than local changes in environment. Therefore, the various shifts allows a much more detailed correlation than can be achieved by carbon isotope stratigraphy (Table 1). Even though some of these correlations are tentative, they are stratigraphically consistent and indicate that the dinocyst assemblage changes reflect environmental change on a regional scale. According to this correlation, events D through K occur within 2 m at Bass River but span ~6 m at Wilson Lake, indicating condensation at Bass River relative to Wilson Lake during the time of deposition (Fig. 4). Moreover, at Wilson Lake, the 2 Myr hiatus occurs approximately 1 m above event N, while the PETM continues for another 6 m at Bass River. This implies that more of the PETM is present at Bass River than at Wilson Lake.

3.3   Statistical analyses

The similarity in dinocyst assemblages between Wilson Lake and Bass River is confirmed by the PCA analyses on relative abundances (Fig. 5a). For both sites the PCAs clearly separate *Areoligera*, *Apectodinium* and *Senegalinium* cpxs. along axes 1 and 2. Also most other taxa mutually plot in similar directions, e.g., Goniodomids and *Operculodinium* plot into a similar direction as *Areoligera*. For further comparison between the sites, we carried out a PCA combining the Wilson Lake and Bass River data (Fig. 5b) and included the sample scores of Axis 1 and Axis 2 in Fig. 2a and b. The patterns in this PCA are similar to the PCAs of the individual sites.

CCA analyses also show congruent patterns between Wilson Lake and Bass River (Fig. 6). At both sites, *Areoligera* as well as *H. tubiferum* (although abundances are relatively low in the assemblages for the latter) plot along wt% >63 fraction. At Bass River, the low-salinity-tolerant group plots very close to magnetic susceptibility. *Apectodinium* generally plots in the same direction as TEX_{86}, although the correlation is not very firm.

4 Discussion

4.1 *Apectodinium* paleoecology

The biotic response of dinocysts to the PETM is particularly interesting because it includes a quasi global acme of, *Apectodinium* spp., thereby comprising usually >40% of the dinocyst assemblage (Heilmann-Clausen, 1985; Powell et al., 1996; Bujak and Brinkhuis, 1998; Heilmann-Clausen and Egger, 2000). Such a global, synchronous acme is unique in the dinocyst fossil record, which spans the late Triassic to the Recent.

4.1.1 Temperature

In the CCA's, *Apectodinium* correlates best with temperature and plots in different directions than the low-salinity-tolerant group, and the inner neritic *Areoligera* cpx. The taxon *Apectodinium* originated close to the Danian-Selandian boundary (Brinkhuis et al., 1994), and abundant occurrences remained largely restricted to low latitudes throughout the Palaeocene (Bujak and Brinkhuis, 1998). It has been hypothesized that temperate to polar sea surface temperatures increased to allow poleward migration of *Apectodinium* during the PETM (Bujak and Brinkhuis, 1998; Crouch et al., 2001; Sluijs et al., 2006). However, recently it was shown that temperatures in mid-latitude regions, incl. New Jersey, were probably already high enough during the Late Paleocene to allow for abundant *Apectodinium* (Zachos et al., 2006; Sluijs et al., 2007b). This indicates that factors other than temperature prevented mid-latitude abundances of this taxon (Sluijs et al., 2007b). Moreover, the onset of the *Apectodinium* acme in New Jersey started prior to the onset of the rise in mean annual temperature (MAT), suggesting that (an) additional environmental factor(s) triggered the acme in this region (Sluijs et al., 2007b). However, the seasonally blooming lifestyle of many dinoflagellates (e.g., Dale, 2001) also keeps open the possibility that warming/stratification in the critical season, thereby not significantly influencing MAT, initiated proliferation of *Apectodinium*. In effect, there is the option that the apparently massive abundance actually

A dynamic climate state during the Paleocene-Eocene Thermal Maximum

A. Sluijs and H. Brinkhuis

Title Page

Abstract | Introduction

Conclusions | References

Tables | Figures

|◄ | ►|

◄ | ►

Back | Close

Full Screen / Esc

Printer-friendly Version

Interactive Discussion

only reflects 2–3 anomalous weeks per year.

4.1.2 Salinity

Most representatives of *Apectodinium* were likely also euryhaline, although truly brackish conditions were perhaps not optimal (Sluijs et al., 2007b, 2008b). While in mid-latitude regions *Apectodinium* contributes at least 40% of the assemblage for much of the PETM (Figs. 2, 3) (Heilmann-Clausen, 1985; Powell et al., 1996; Bujak and Brinkhuis, 1998; Heilmann-Clausen and Egger, 2000), *Apectodinium* abundances only reach to ∼20% in the Arctic, where typical low-salinity-tolerant dinocysts remain dominant (Sluijs et al., 2008b). Similar trends are recorded at Bass River and Wilson Lake, where *Apectodinium* spp. became outnumbered by typical low-salinity-tolerant dinocysts during phases of the PETM (Figs. 2, 3). Moreover, *Apectodinium* spp. do not plot closely to the low-salinity-tolerant dinocysts in the PCA. This indicates that while *Apectodinium* was reasonably successful at relatively low salinities, such as in the Arctic during the PETM (Sluijs et al., 2008b), other taxa were able to dominate dinocyst assemblages under such ecological conditions.

4.1.3 Heterotrophy

Several authors have suggested that the dinoflagellates that formed *Apectodinium* cysts were heterotrophic and fed on organic detritus or other plankton (Bujak and Brinkhuis, 1998). This suggestion was primarily based on the fact that *Apectodinium* exhibits the same basic plate organization, a critical tool in taxonomical classification, as the Modern heterotrophic, mainly diatom feeding (Buskey, 1997) genus *Protoperidinium*, suggesting that they are related. Moreover, the pentagonal outline of *Apectodinium* fossils is in the modern ocean only found in *Protoperidinium* (sub)fossils.

At both Wilson Lake and Bass River we have recorded many *Apectodinium* specimens that have the typical brown color usually observed in cysts of Modern members of *Protoperidinium* (Plate 1I–L). This implies that, along with the systematic resem-

blances, the material of the *Apectodinium* cysts is very similar to Modern *Protoperidinium* fossils, further corroborating the notion that *Apectodinium* was a heterotrophic dinoflagellate.

Its presumed heterotrophic lifestyle implies that *Apectodinium*, similar to Modern *Protoperidinium*, was dependent on the availability of prey (perhaps diatoms, or other (even zoo-) plankton) that are, in turn, dependent on nutrient availability (particularly nitrogen and phosphorus). Hence, the global nature of the *Apectodinium* acme during the PETM (Sluijs et al., 2007a) suggests that shallow seas around the globe exhibited a strong increase in nutrient availability, or some food source (Powell et al., 1996; Bujak and Brinkhuis, 1998; Crouch et al., 2001, 2003a; Crouch and Brinkhuis, 2005; Sluijs et al., 2005). Locally, elevated near-coast productivity at the PETM has been suggested to explain benthic foraminifer and calcareous nannofossil assemblage changes as well as organic rich sediments in marginal marine realms (e.g., Thomas and Shackleton, 1996; Speijer and Schmitz, 1998; Gavrilov et al., 2003; Gibbs et al., 2006; Sluijs et al., 2006; see overview in Sluijs et al., 2007, 2008b).

The mechanism behind global eutrophication of at least shallow seas is as yet unclear. It has been suggested that the global warming associated with the PETM triggered intensification of weathering, the hydrological cycle and run off at many regions in the world (Robert and Kennett, 1994; Ravizza et al., 2001; Schmitz et al., 2001; Crouch et al., 2003b; Hollis et al., 2005; Giusberti et al., 2007; Nicolo et al., 2007; Sluijs et al., 2007b). Alternatively, modeling studies have suggested intensification of storms in an extreme greenhouse world (Emanuel, 2005; Emanuel et al., 2004; Sriver and Huber, 2007). If more intense storms occurred during the PETM compared to background conditions, they should have regionally caused mixing of deeper nutrient rich waters into the photic zone, thereby promoting primary production.

Because the fossil record only represents a very small part of the surface water organisms, it is hard to reconstruct a relatively complete food web for the PETM. Therefore it is equally difficult to identify the exact food source of *Apectodinium*. Regardless of these unanswered questions on its nature, the acme directly implies that the food

source of *Apectodinium* was globally very abundant in shallow marine settings.

4.1.4 Which other critical factor?

A baseline requirement for the distribution of *Apectodinium* appears to have been high temperatures. *Apectodinium* acmes have been recorded from upper Paleocene deposits in the Tethyan Ocean (Iakovleva et al., 2001), suggesting that conditions there were episodically and locally similar to those on a global scale during the PETM (Crouch et al., 2003a). Similar to other mid-latitude regions, *Apectodinium* was already present on the New Jersey Shelf at least since Chron C25n times (Fig. 2); yet, in contrast to low-latitude sites (Iakovleva et al., 2001) no pre-PETM acmes have been reported from such regions. Moreover, food availability and salinity, and/or stratification seem important. Although the above parameters were likely important for the distribution of *Apectodinium*, it appears that even a combination of these factors was likely not truly unique in the early Paleogene at mid latitudes. This suggests that some critical other environmental factor(s) that stimulated massive *Apectodinium* production, has not yet been identified. Somehow, however, this unidentified factor was related to the PETM. Whichever combination of surface water parameters caused the global acme of *Apectodinium*, it is consistently associated with the PETM and appears to signify a harbinger to global warming and carbon injection as the acme started just prior to the PETM warming and the CIE in mid-latitude areas (Sluijs et al., 2007b).

4.2 *Areoligera* and transgression

Much empirical evidence suggests that a dominance of the *Areoligera* cpx indicates inner neritic, high energy environments (Brinkhuis, 1994; Pross and Brinkhuis, 2005), while the *Spiniferites* cpx is mostly recorded from neritic deposits with increasing relative abundances at outer neritic localities (Brinkhuis, 1994; Pross and Brinkhuis, 2005). This evidence was previously used to infer an Upper Paleocene transgression in New Jersey by applying the ratio between *Spiniferites* and *Areoligera* abundances (Sluijs et

Title Page

Abstract | Introduction

Conclusions | References

Tables | Figures

◄ | ►

◄ | ►

Back | Close

Full Screen / Esc

Printer-friendly Version

Interactive Discussion

al., 2008a). In the CCA analyses (Fig. 6), *Areoligera* shows a significant correlation with the wt% coarse fraction of the sediment, which had been previously been used to identify a phase of transgression (Liu et al., 1997; Cramer et al., 1999). *Spiniferites* does not correlate to any proxy data in the CCAs, supporting the inference that they in-
5 habited all areas on the shelf during the Paleogene, much like today (Wall et al., 1977). Abundant *Areoligera* appears in New Jersey, and also in other regions (e.g., Crouch and Brinkhuis, 2005; Iakovleva et al., 2001; Sluijs et al., 2008a) consistently related to third order transgressive systems tracts in sequence stratigraphic terms, and thus sea level rise in neritic settings.
10 Hence, similar to the *Spiniferites/Aeroligera* ratio (Sluijs et al., 2008a), the sample scores for axis 1 of the PCA at Bass River and Wilson Lake should in part reflect sea level (Fig. 2). The recorded trends are consistent with a transgression during the PETM, a phenomenon recorded on a global scale (Sluijs et al., 2008a).

4.3 Fresh water forcing

15 Axis 2 in all PCAs is dominated by the abundances of the low-salinity-tolerant group, making it an indicator for low salinity. In the CCA, low-salinity-tolerant group corresponds closely to magnetic susceptibility of the sediment at Bass River. The MS values are dominantly controlled by abundances of biogenic magnetic particles, produced by bacteria (Kopp et al., 2007; Lippert and Zachos, 2007). These bacteria thrive in
20 a particular niche, as they require low oxygen concentrations and a high supply of iron (Fe^{2+}). But conditions were not euxinic because free sulfide dissolves bacterial magnetite (Canfield and Berner, 1987; Dickens, 2008). These specific requirements suggest that high fluxes of organic carbon to the sea floor, together with the PETM warming, decreased the oxygen content of pore waters, while high clay fluxes that
25 were deposited on top of pore waters that still contained some oxygen prevented the establishment of euxinia (Dickens, 2008). This requires a significant increase in runoff and production rates (Lippert and Zachos, 2007), which is consistent with the strong positive correlation between MS and the *Senegalinium* cpx, which not only evidences

low salinities, but also high food/nutrient supply (Sluijs et al., 2007b).

This supports previous inferences (Brinkhuis et al., 2006; Sluijs et al., 2006, 2007b, 2008b) that many hexa-peridinioids, particularly *Senegalinium* and *Phthanoperidinium*, but also *Deflandrea*, *Cerodinium, Spinidinium* and related genera (Sluijs et al., 2009), were indeed tolerant to low salinities and flourished best during episodes of abundant food (e.g., Dale and Fjellså, 1994; Firth, 1996; see overview in Sluijs et al., 2005). Abundances of the *Senegalinium* cpx suggest that increased fresh water forcing started some time (perhaps 10 kyr, if the cycles in *Apectodinium* (Fig. 2) are precession-related (Sluijs et al., 2007b), see below) after the onset of the CIE, consistent with a humid climate state at least during the first ~100 kyr of the PETM (e.g., Bowen et al., 2004).

5   A variable climate state during the PETM?

Although high abundances of *Apectodinium* and *Senegalinium* occur across portions of the New Jersey PETM sections, abundances clearly vary significantly during the PETM. Short-lived acmes of *Hystrichosphaeridium*, *Eocladopyxis* spp., *Cordosphaeridium fibrospinosum*, *Membranosphaera* spp. and a new species of *Florentinia* occur throughout the PETM at both Bass River and Wilson Lake. Such variation is absent in the sediments deposited during the ~1 Ma prior to the PETM. In part, this may be related to winnowing, indicated by the general low abundance of clay and the coarse nature of the sediments, which would concentrate the relatively large taxon *Areoligera* and reduce abundances of smaller taxa, particularly *Senegalinium* spp., *Phthanoperidinium* spp. and *Membranosphaera* spp. However, the absence of temporal abundances of other typically large taxa, such as specimens of *Cordosphaeridium* and *Hystrichosphaeridium*, as recorded within the PETM, suggests more stable conditions prior to than during the event.

The cyclic abundances of *Apectodinium* as recorded within the PETM at Bass River, both as a percentage of the assemblage and numbers per gram sediment, has been

suggested to be associated to the orbital cycle of precession (Sluijs et al., 2007b). Regardless of the forcing mechanism, maxima in *Apectodinium* co-occur with maxima in the number of total dinocysts per gram sediment. The cyclic behaviour of total dinocysts and *Apectodinium* per gram, while absolute abundances of most other taxa remain constant, strongly suggests nutrient/food supply as a cause rather than variations in siliciclastic sediment supply. Assuming constant preservation, which is likely considering persistent suboxic seafloor conditions (Dickens, 2008; Kopp et al., 2007; Lippert and Zachos, 2007), varying nutrient/food abundances controlled the cycles in *Apectodinium*, consistent with a heterotrophic lifestyle of this taxon.

Peak abundances of representatives of *Eocladopyxis*, a genus within the family of Goniodomaceae that in the Modern is usually associated with low latitude hyposaline or hypersaline lagoonal settings (Bradford and Wall, 1984; Wall et al., 1977), are temporally recorded close to the onset of the PETM at both Bass River and Wilson Lake. Perhaps these taxa have been transported down the shelf from lagoonal settings, but persistent low abundances of terrestrial organic matter (palynomorphs or biomarkers) invokes another mechanism. High abundances of the related taxon *Polysphaeridium zoharyi* have been recorded in the central Arabian Sea following North Atlantic Heinrich events (Reichart et al., 2004). These abundances were explained by a mechanism of regional warming in winter, preventing a saline surface layer to overturn, causing a 'hyperstratified' situation with lagoonal-type conditions in the open ocean (Reichart et al., 2004). Analogously, the establishment of seasonal hyperstratification, with hypersaline and warm surface waters, could explain temporal *Eocladopyxis* abundances on the New Jersey shelf.

Abundances of *Cordosphaeridium fibrospinosum* and (a large group of) related taxa by several authors often informally referred to as the *C. fibrospinosum* complex of morphologically highly variable taxa (see taxonomic section) abundantly occur during intervals within the PETM at Bass River and Wilson Lake. Although this complex as a whole has gone extinct, it was cosmopolitan and several taxa within this group have been associated with stratified and even brackish conditions (e.g., Pross, 2001;

A dynamic climate state during the Paleocene-Eocene Thermal Maximum

A. Sluijs and H. Brinkhuis

Houben, 2008). *Hystrichosphaeridium* is also temporally abundant and our CCA analyses plot this species together with *Areoligera* towards wt% coarse fraction, suggesting it thrived in relatively high-energy environments. Only few paleoecological information is available for *Membranosphaera*, although it seems most abundant in higher latitudes (sometimes called *Elytrocysta* in Southern Ocean sections, (e.g., Brinkhuis et al., 2003; Sluijs et al., 2003) and tolerated relatively low salinities (Sluijs et al., 2008b). Even less information is available for the new species *Florentinia reichartii* apart from that we have recorded it in marginal marine upper Paleocene – lower Eocene sediments in the Gulf of Mexico and the southwest Pacific we are currently studying (personal observation).

6 Synthesis/concluding remarks

Our findings prompt a picture of high environmental variability during the PETM at the New Jersey Shelf, likely related to at least regional climatic variability. Our results strongly suggest that the bulk of the variation we note is due to regional precipitation and runoff fluctuations, rather than the overall warm temperature. Such fluctuations may have led to strong, coupled stratification and salinity changes that may have guided the subsequent abundances of, e.g., the *Senegalinium, Membranosphaera*, and Goniodomid groups, *Hystrichosphaeridium* and *F. reichartii.* The hydrological cycle during the "ultra greenhouse" was apparently highly unstable, at least on a regional scale and on milankovitch time scales. In this light, it is also remarkable that the relative and absolute abundance of sporomorphs from terrestrial higher plants is low during the PETM in New Jersey. Other mid latitude PETM sites around the world do yield sometimes even stunning amounts of pollen and spores (e.g., Crouch et al., 2003b; Harrington, 2003; Steurbaut et al., 2003). One speculation concerning this aspect is that the hydrological or temperature regime of the region was so extreme that no stable vegetation could be established during this time.

This study also indicates the necessity of analyzing more chronostratigraphically well

calibrated, high accumulation PETM marine, and also terrestrial sites around the world, principally to determine if the New Jersey climatic variability during the PETM was a regional or larger scaled phenomenon.

7 Taxonomy

7.1 Systematic paleontology

Division Dinoflagellata (Bütschli, 1885); Fensome et al. (1993)
Class Dinophyceae Pascher (1914)
Subclass Peridiniphycidae Fensome et al. (1993)
Order Gonyaulacales Taylor (1980)
Family Gonyaulaceae Lindemann (1928)
Subfamily Cribroperidinioideae Fensome et al. (1993)

Florentinia reichartii sp. nov.
Plate 3, F–L; Plate 4, A–C

Derivation of name: Named for Gert-Jan Reichart, geochemist at Utrecht University, in recognition of his pioneer integrated geochemical and palynological studies.

Holotype: Plate 4, A–C. Specimen with numerous hollow processes, an antapical horn (4A), and an archeopyle involving precingular plate 3" (4A–B) plus all apical plates (see sulcal notch, 4C); paratypes: Plate 3, F–G, H–I, J, K–L.

Diagnosis: A small species of *Florentina* with distally closed, hollow, long cone-shaped processes and a short, blunt antapical horn.

Description: Small, chorate gonyaulacean cysts, characterized by a small antapical

A dynamic climate state during the Paleocene-Eocene Thermal Maximum

A. Sluijs and H. Brinkhuis

horn, and an archeopyle that involves all apical and sometimes precingular plates. Operculum usually free, but may be partially attached. Central body is psilate and almost transparent. Processes are long, approximately (or sometimes more than) half the size of the central body, are hollow and distally-closed and non-tabular. Some
5 processes may fuse in proximity of the central body. The antapical horn is relatively short, approximately as wide as long, and often barely visible. Tabulation is barely discernable, either (1) by some degree of clustering of groups of processes, besides the (2) antapical horn reflecting 6"" , and usually constituting the only consistent marker for orientation. The archeopyle can only rarely be positively identified as type
10 tA, and may additionally involve plate 4", with usually a detached operculum.

Discussion: *Florentinia reichartii* can be easily confused with *Lingulodinium machaerophorum* or *Diphyes* spp. during microscope analyses, but these are both usually larger and have precingular archeopyles, while *L. machaerophorum* also lacks
15 an antapical horn. *F. reichartii* is much smaller than most other species within the genus, and its antapical horn is small relative to the size of the central body. Within the genus *Florentinia*, it bears closest resemblance to the much larger *F. ferox*, because processes may also fuse in proximity of the central body to create process-complexes. *F. ferox*, however, which has more proximally united processes that reflect tabulation,
20 rather than clustered individual processes.

Dimensions: Holotype: 23×28 μm. Range: length 20(23)25 μm, breadth 23(24)28 μm. Specimens measured 10.

25 **Stratigraphic occurrence**: Latest Paleocene and earliest Eocene on the New Jersey Shelf (upper Vincetown and Manasquan formations), northern plain of the Gulf of Mexico (Alabama, Missisippi), East Tasman Plateau (Ocean Drilling Program Leg 189).

7.2 List of encountered dinocyst species and complexes

The generic allocation of taxa follows that cited in Fensome and Williams (2004) unless stated otherwise. Along with *Florentinia reichartii* sp. nov., some new taxa have been recorded and are discussed below, and will be formally described elsewhere. Notes on certain taxa are also provided. Illustrated taxa are followed by plate references in brackets.

Achilleodinium biformoides (1A–B)
Achomosphaera alcicornum (1C)
Achomosphaera crassipellis
Adnatosphaeridium multispinosum
Adnatosphaeridium robustum (1D–F; 9A)
Alisocysta sp. 2 of Heilmann-Clausen (1985)
Apectodinium augustum (1I)
Apectodinium homomorphum Remarks: variation with very long processes abundant (1J; 9B–C)
Apectodinium parvum (1K)
Apectodinium quinquelatum Remarks: variation with very long processes abundant (1L)
Apteodinium spp.
Areoligera coronata
Areoligera senonensis
Areoligera cpx. This complex includes the morphologically closely related, 'dorsal-ventrally compressed Gonyaulacoid' genera *Areoligera, Glaphyrocysta* and *Adnatosphaeridium* (9D)
Batiacasphaera compta
Batiacasphaera spp. (pars). Other species of *Batiacasphaera*
Calligodinium aceras
Cerebrocysta spp. (9E)

A dynamic climate state during the Paleocene-Eocene Thermal Maximum

A. Sluijs and H. Brinkhuis

Title Page

Abstract Introduction

Conclusions References

Tables Figures

◄ ►

◄ ►

Back Close

Full Screen / Esc

Printer-friendly Version

Interactive Discussion

A dynamic climate state during the Paleocene-Eocene Thermal Maximum

A. Sluijs and H. Brinkhuis

Cerodinium denticulatum
Cerodinium depressum
Cerodinium speciosa
Cerodinium wardenense

5 *Cladopyxidium saeptum* (2A)

Cordosphaeridium fibrospinosum (2B–E; 9F–G)

Cordosphaeridium fibrospinosum cpx. Several authors (e.g., Brinkhuis and Schiøler, 1996) have discussed the morphologically closely related genera *Apteodinium*, *Cordosphaeridium, Damassadinium, Fibrocysta*, *Kenleya*. *Lanternosphaeridium*, *Murato-*

10 *dinium*, *Thalassiphora*, and *Turbiosphaera*, and even others. The "plasticity" in specimens assignable to this group is horrific and virtually any morphological intermediate between several types of genera may be readily identified in Upper Palaeocene and Early Eocene assemblages. Following Brinkhuis and Schioler (1996), we have chosen *C. fibrospinosum* as a central taxon in this group. Ongoing studies (e.g., Houben,

15 2008), indicate that many of the morphological manifestations recorded within this complex may in fact represent a single biological species, yet with different morphological end-members through geological time.

Cordosphaeridium miminum

Cribroperidinium sp. A. An unusual, very large (∼100 μm), thin-walled species

20 of *Cribroperidinium*. Tabulation only discernible at cingulum and through the 4" archeopyle; operculum detached. (2H)

Cribroperidinium spp (pars.). Other species of Cribroperidinium

Damassadinium spp. Part of the *C. fibrospinosum* cpx

Dapsilidinium spp.

25 *Deflandrea oebisfeldensis* (2I)

Deflandrea phosphoritica

Diphyes colligerum (2J; 9H)

Dracodinium pachydermum (2K)

Dracodinium varielongitudum (8C)

Eocladopyxis peniculata (3A–B; 9I–L))

Eocladopyxis? sp. A. A proximate Goniodomid, questionably assigned to *Eocladopyxis*

Fibrocysta axialis (10A) Part of the *C. fibrospinosum* cpx

Fibrocysta bipolaris Part of the *C. fibrospinosum* cpx

5   *Fibrocysta* sp. A. A species of *Fibrocysta* with numerous slender processes Part of the *C. fibrospinosum* cpx

Fibrocysta spp. (pars). All other taxa assignable to *Fibrocysta* (3C) Part of the *C. fibrospinosum* cpx

Florentinia ferox (3D–E)

10 *Florentinia reichartii* sp. nov. (3D–L; 4A–C; 10B–E)

Glaphyrocysta ordinata

Glaphyrocysta pastielsii/exuberans

Glaphyrocysta reticulata

Glaphyrocysta volata (3D–E; 10F–G)

15 *Hafniasphaera septata*(3F–G)

Heteraulacacysta spp. (3H–I)

Homotryblium spp. (3J–K)

Horologiniella spp.

Hystrichokolpoma salacia (5A–C)

20 *Hystrichokolpoma* spp. (pars)

Hystrichosphaeridium truswelliae Remarks: first record outside Southern Ocean. (5D–F; 10H–I)

Hystrichosphaeridium tubiferum

Hystrichostrogylon spp. (5G)

25 *Impagidinium californiense*

Impagidinium sp. cf. *I.* sp. B Crouch and Hollis (1996)

Impagidinium sp. cf. *sphaericum*

Impagidinium spp. (pars)

Kallosphaeridium brevibarbatum

A dynamic climate state during the Paleocene-Eocene Thermal Maximum

A. Sluijs and H. Brinkhuis

Title Page

Abstract   Introduction

Conclusions   References

Tables   Figures

◄   ►►

◄   ►

Back   Close

Full Screen / Esc

Printer-friendly Version

Interactive Discussion

Kenleya spp.
Lanternosphaeridium lanosum (5H–I; 10J). Part of the *C. fibrospinosum* cpx
Lejeunecysta spp.
Leptodinium spp.
5 *Lingulodinium machaerophorum*
Melitasphaeridium pseudorecurvatum
Membranosphaera spp. Remarks: tabulation sometimes discernable in process orna-
mentation (5K; 10K)
Microdinium ornatum
10 *Muratodinium fimbriatum* (6A–B; 10L). Part of the *C. fibrospinosum* cpx
Nelsoniella (Reworked; 8F)
Nematosphaeropsis spp.
Operculodinium severinii
Operculodinium cf. *O. israelianum.*
15 *Operculodinium* spp. (pars) (6C–D; 11A)
Paleocystodinium lidiae
Paleocystodinium spp. (pars) (11B)
Paleotetradinium minisculum (6E)
Paucisphaeridium inversibuccinum
20 *Paucisphaeridium* spp. (pars) (6F–G; 11C)
Phelodinium magnificum (6H–I)
Phthanoperidinium crenulatum (6J–L; 11D–F)
Phthanoperidium spp. (pars)
Polysphaeridium zoharyi (7A–B)
25 *Rhombodinium* spp. (7C–D)
Rottnestia borussica (7E)
Selenopemphix nephroides (7F)
Senegalinium spp. (7G–H)

Senegalinium cpx. Includes all peridinioid taxa with a 6-sided second intercalary plate; here comprising *Alterbidinium* spp., *Cerodinium* spp., *Deflandrea* spp., *Phthanoperidinium* spp., and *Senegalinium* spp.

Spiniferites pseudofurcatus

5   *Spiniferites ramosus*

Spiniferites spp. (pars)

Tanyosphaeridium spp. (7I)

Thalassiphora delicata (7J–L)

Thalassiphora pelagica. Part of the *C. fibrospinosum* cpx

10   *Turbiosphaera* spp. Part of the *C. fibrospinosum* cpx

Wetzeliella articulata (8A–B)

Wetzeliella meckelfeldensis

Wilsonidium tesselatum (8D–E)

◄◄   ►►

◄   ►

Back   Close

Full Screen / Esc

Printer-friendly Version

Interactive Discussion

References

Abdul Aziz, H., Hilgen, F. J., van Luijk, G. M., Sluijs, A., Kraus, M. J., Pares, J. M., and Gingerich, P. D.: Astronomical climate control on paleosol stacking patterns in the upper Paleocene – lower Eocene Willwood Formation, Bighorn Basin, Wyoming, Geology, 36, 531–534, doi:10.1130/G24734A.1, 2008.

Archer, D.: Fate of fossil fuel CO_2 in geologic time, J. Geophys. Res., 110, doi:10.1029/2004JC002625, 2005.

Bowen, G. J., Beerling, D. J., Koch, P. L., Zachos, J. C., and Quattlebaum, T.: A humid climate state during the Palaeocene/Eocene thermal maximum, Nature, 432, 495–499, 2004.

Bowen, G. J., Bralower, T. J., Delaney, M. L., Dickens, G. R., Kelly, D. C., Koch, P. L., Kump, L. R., Meng, J., Sloan, L. C., Thomas, E., Wing, S. L., and Zachos, J. C.: Eocene Hyperthermal Event Offers Insight Into Greenhouse Warming, EOS, Transactions, American Geophysical Union, 87, 165, 169, 2006.

Bradford, M. R. and Wall, D. A.: The Distribution of Recent Organic-Walled Dinoflagellate Cysts in the Persian Gulf, Gulf of Oman, and northwestern Arabian Sea, Palaeontographica, 192, 16–84, 1984.

Brinkhuis, H.: Late Eocene to Early Oligocene dinoflagellate cysts from the Priabonian type-area (Northeast Italy); biostratigraphy and palaeoenvironmental interpretation, Palaeogeogr. Palaeocl., 107, 121–163, 1994.

Brinkhuis, H., Romein, A. J. T., Smit, J., and Zachariasse, W. J.: Danian-Selandian dinoflagellate cysts from lower latitudes with special reference to the El Kef section, NW Tunesia, Geologiska Föreningens i Stockholm Förhandlingar (GFF; Transactions of the Geological Society in Stockholm), 116, 46–48, 1994.

Brinkhuis, H. and Schiøler, P.: Palynology of the Geulhemmerberg Cretaceous/Tertiary boundary section (Limburg, SE Netherlands), Geologie en Mijnbouw, 75, 193–213, 1996.

Brinkhuis, H., Sengers, S., Sluijs, A., Warnaar, J., and Williams, G. L.: Latest Cretaceous to earliest Oligocene, and Quaternary dinoflagellate cysts from ODP Site 1172, East Tasman Plateau, in: Proceedings Ocean Drilling Program, Scientific Results, edited by: Exon, N. F., Kennett, J. P., and Malone, M., College Station, Texas, 1–48, 2003.

Bujak, J. P. and Brinkhuis, H.: Global warming and dinocyst changes across the Paleocene/Eocene Epoch boundary, in: Late Paleocene – early Eocene climatic and biotic events in the marine and terrestrial records, edited by: Aubry, M.-P., Lucas, S. G., and Berggren, W.

A dynamic climate state during the Paleocene-Eocene Thermal Maximum

A. Sluijs and H. Brinkhuis

A., Columbia University Press, New York, 277–295, 1998.

Buskey, E. J.: Behavioral components of feeding selectivity of the heterotrophic dineflagellate Protoperidinium pellucidum, Mar. Ecol.-Prog. Ser., 153, 77–89, 1997.

Bütschli, O.: Protozoa, in: Klassen und Ordnungen des Thier-Reichs, Wissenschaftlich Dargestellt in Wort und Bild, edited by: Bronn, H. G., Wintersche Verlagsbuchhandling, Leibzig, 865–1088, 1885.

Canfield, D. E. and Berner, R. A.: Dissolution and pyritization of magnetite in anoxie marine sediments Geochimica, Cosmochimica Acta, 51, 1987.

Cramer, B. S., Aubry, M.-P., Miller, K. G., Olsson, R. K., Wright, J. D., and Kent, D. V.: An exceptional chronologic, isotopic, and clay mineralogic record of the latest Paleocene thermal maximum, Bass River, NJ, ODP 174AX, B. Soc. Geol. Fr., 170, 883–897, 1999.

Crouch, E. M. and Hollis, C. J.: Paleogene palynomorph and radiolarian biostratigraphy of DSDP Leg 29, sites 280 and 281 South Tasman Rise, 1996.

Crouch, E. M., Heilmann-Clausen, C., Brinkhuis, H., Morgans, H. E. G., Rogers, K. M., Egger, H., and Schmitz, B.: Global dinoflagellate event associated with the late Paleocene thermal maximum, Geology, 29, 315–318, 2001.

Crouch, E. M., Brinkhuis, H., Visscher, H., Adatte, T., and Bolle, M.-P.: Late Paleocene- early Eocene dinoflagellate cyst records from the Tethys: Further observations on the global distribution of *Apectodinium*, in: Causes and Consequences of Globally Warm Climates in the Early Paleogene, Geological Society of America Special Paper 369, edited by: Wing, S. L., Gingerich, P. D., Schmitz, B., and Thomas, E., Geological Society of America, Boulder, Colorado, 113–131, 2003a.

Crouch, E. M., Dickens, G. R., Brinkhuis, H., Aubry, M.-P., Hollis, C. J., Rogers, K. M., and Visscher, H.: The *Apectodinium* acme and terrestrial discharge during the Paleocene-Eocene thermal maximum: new palynological, geochemical and calcareous nannoplankton observations at Tawanui, New Zealand, Palaeogeogr. Palaeocl.,194, 387–403, 2003b.

Crouch, E. M. and Brinkhuis, H.: Environmental change across the Paleocene-Eocene transition from eastern New Zealand: A marine palynological approach, Mar. Micropaleontology, 56, 138–160, 2005.

Dale, B. and Fjellså, A.: Dinoflagellate cysts as paleoproductivity indicators: State of the art, potential and limits, in: Carbon Cycling in the Glacial Ocean: Constraints on the Ocean's Role in Global Change, edited by: Zahn, R., Pedersen, T. F., Kaminski, M. A., and Labeyrie, L., Springer, Berlin, 521–537, 1994.

A dynamic climate state during the Paleocene-Eocene Thermal Maximum

A. Sluijs and H. Brinkhuis

Dale, B.: The sedimentary record of dinoflagellate cysts: looking back into the future of phytoplankton blooms, Scientia Marina, 2, edited by: Gili, J. M., Pretus, J. L., and Packard, T. T., 257–272, 2001.

Dickens, G. R., O'Neil, J. R., Rea, D. K., and Owen, R. M.: Dissociation of oceanic methane hydrate as a cause of the carbon isotope excursion at the end of the Paleocene, Paleoceanography, 10, 965–971, 1995.

Dickens, G. R., Castillo, M. M., and Walker, J. C. G.: A blast of gas in the latest Paleocene: Simulating first-order effects of massive dissociation of oceanic methane hydrate, Geology, 25, 259–262, 1997.

Dickens, G. R.: The riddle of the clays, Nature Geoscience, 1, 86–88, 2008.

Diffenbaugh, N. S., Giorgi, F., and Pal, J. S.: Climate change hotspots in the United States, Geophys. Res. Lett., doi:10.1029/2008GL035075, 2008.

Egger, H., Fenner, J., Heilmann-Clausen, C., Rögl, F., Sachsenhofer, R., and Schmitz, B.: Paleoproductivity of the northwestern Tethyan margin (Anthering section, Austria) across the Paleocene-Eocene transition, in: Causes and Consequences of Globally Warm Climates in the Early Paleogene, Geological Society of America Special Paper 369, edited by: Wing, S. L., Gingerich, P. D., Schmitz, B., and Thomas, E., Geological Society of America, Bolder, Colorado, 133–146, 2003.

Ellegaard, M.: Variations in dinoflagellate cyst morphology under conditions of changing salinity during the last 2000 years, Rev. Palaeobot. Palyno., 109, 65–81, 2000.

Emanuel, K., DesAutels, C., Holloway, C., and Korty, R.: Environmental Control of Tropical Cyclone Intensity, J. Atmos. Sci., 61, 843–858, 2004.

Emanuel, K.: Increasing destructiveness of tropical cyclones over the past 30 years, Nature, 436, 686–688, 2005.

Fensome, R. A., Taylor, F. J. R., Norris, G., Sarjeant, W. A. S., Wharton, D. I., and Williams, G. L.: A Classification of Fossil and Living Dinoflagellates, Micropaleontology Special Publication, no. 7, 351 pp., 1993.

Fensome, R. A., Gocht, H., and Williams, G. L.: The Eisenack Catalog of Fossil Dinoflagellates, New Series, 4, E. Schweizerbart'sche Verlagsbuchhandlung, Stuttgart, Germany, 2009–2548, 1996.

Fensome, R. A. and Williams, G. L.: The Lentin and Williams Index of Fossil Dinoflagellates 2004 Edition, American Association of Stratigraphic Palynologists (AASP) Contribution Series 42, 909 pp., 2004.

A dynamic climate state during the Paleocene-Eocene Thermal Maximum

A. Sluijs and H. Brinkhuis

Title Page

Abstract | Introduction

Conclusions | References

Tables | Figures

|◄ | ►|

◄ | ►

Back | Close

Full Screen / Esc

Printer-friendly Version

Interactive Discussion

Gibbs, S. J., Bralower, T. J., Bown, P. R., Zachos, J. C., and Bybell, L. M.: Shelf and open-ocean calcareous phytoplankton assemblages across the Paleocene-Eocene Thermal Maximum: Implications for global productivity gradients, Geology, 34, 233–236, 2006.

Gibson, T. G., Bybell, L. M., and Owens, J. P.: Latest Paleocene lithologic and biotic events in neritic deposits of Southwestern New Jersey, Paleoceanography, 8, 495–514, 1993.

Gibson, T. G., Bybell, L. M., and Mason, D. B.: Stratigraphic and climatic implications of clay mineral changes around the Paleocene/Eocene boundary of the northeastern US margin, Sediment. Geol., 134, 65–92, 2000.

Giusberti, L., Rio, D., Agnini, C., Backman, J., Fornaciari, E., Tateo, F., and Oddone, M.: Mode and tempo of the Paleocene-Eocene thermal maximum in an expanded section from the Venetian pre-Alps, Geol. Soc. Am. Bull., 119, 391–412, 2007.

Hallett, R. I.: Consequences of Environmental Change on the Growth and Morphology of *Lingulodinium polyedrum* (Dinophyceae) in Culture, Ph.D., University of Westminster, London, 109 pp., 1999.

Harrington, G. J.: Geographic patterns in the floral response to Paleocene-Eocene warming, in: Causes and Consequences of Globally Warm Climates in the Early Paleogene, edited by: Wing, S. L., Gingerich, P. D., Schmitz, B., and Thomas, E., Geological Society of America Special Paper 369, Boulder, Colorado, 381–393, 2003.

Heilmann-Clausen, C.: Dinoflagellate stratigraphy of the Uppermost Danian to Ypresian in the Viborg 1 borehole, Central Jylland, Denmark, DGU A7, 1–69, 1985.

Heilmann-Clausen, C. and Egger, H.: The Anthering outcrop (Austria), a key-section for correlation between Tethys and Northwestern Europe near the Paleocene/Eocene boundary, in: Early Paleogene Warm Climates and Biosphere Dynamics, edited by: Schmitz, B., Sundquist, B., and Andreasson, F. P., GFF (Geologiska Föreningens Förhandlingar), Geological Society of Sweden, Uppsala, 69, 2000.

Higgins, J. A. and Schrag, D. P.: Beyond methane: Towards a theory for the Paleocene-Eocene Thermal Maximum, Earth Planet. Sc. Lett., 245, 523–537, 2006.

Hollis, C. J., Dickens, G. R., Field, B. D., Jones, C. M., and Percy Strong, C.: The Paleocene-Eocene transition at Mead Stream, New Zealand: a southern Pacific record of early Cenozoic global change, Palaeogeogr. Palaeocl., 215, 313–343, 2005.

Houben, S.: Organic Walled Dinoflagellate Cysts as indicators for environmental change during the Middle Eocene Climatic Optimum (MECO): results from ODP Leg 120, Site 748 (Kerguelen Plateau), M.Sc, Palaeoecology, Institute of Environmental Biology, Utrecht University,

A dynamic climate state during the Paleocene-Eocene Thermal Maximum

A. Sluijs and H. Brinkhuis

Title Page

Abstract | Introduction

Conclusions | References

Tables | Figures

|◄ | ►|

◄ | ►

Back | Close

Full Screen / Esc

Printer-friendly Version

Interactive Discussion

Utrecht, 29 pp., 2008.

Iakovleva, A. I., Brinkhuis, H., and Cavagnetto, C.: Late Palaeocene-Early Eocene dinoflagellate cysts from the Turgay Strait, Kazakhstan; correlations across ancient seaways, Palaeogeogr. Palaeocl., 172, 243–268, 2001.

John, C. M., Bohaty, S. M., Zachos, J. C., Sluijs, A., Gibbs, S. J., Brinkhuis, H., and Bralower, T. J.: North American continental margin records of the Paleocene-Eocene thermal maximum: Implications for global carbon and hydrological cycling, Paleoceanography, 23, PA2217, doi:2210.1029/2007PA001465, 2008.

Kennett, J. P. and Stott, L. D.: Abrupt deep-sea warming, palaeoceanographic changes and benthic extinctions at the end of the Palaeocene, Nature, 353, 225–229, 1991.

Kopp, R. E., Raub, T. D., Schumann, D., Vali, H., Smirnov, A. V., and Kirschvink, J. L.: Magnetofossil spike during the Paleocene-Eocene thermal maximum: Ferromagnetic resonance, rock magnetic, and electron microscopy evidence from Ancora, New Jersey, United States, Paleoceanography, 22, doi:10.1029/2007PA001473, 2007.

Kraus, M. J. and Riggins, S.: Transient drying during the Paleocene-Eocene Thermal Maximum (PETM): Analysis of paleosols in the bighorn basin, Wyoming, Palaeogeogr. Palaeocl., 245, 444–461, 2007.

Lindemann, E.: Abteilung Peridineae (Dinoflagellatae), in: Die Natürlichen Pflanzenfamilien nebst ihren Gattungen und wichtigeren Arten insbesondere den Nutzpflanzen. Zweite stark vermehrte und verbesserte Auflage herausgegeven von A. Engler. 2 Band, edited by: Engler, A. and Prantl, K., Wilhelm Engelmann, Leipzig, Germany, 3–104, 1928.

Lippert, P. C. and Zachos, J. C.: A biogenic origin for anomalous fine-grained magnetic material at the Paleocene-Eocene boundary at Wilson Lake, New Jersey, Paleoceanography, 22, doi:10.1029/2007PA001471, 2007.

Liu, C., Browning, J. V., Miller, K. G., and Olsson, R. K.: Paleocene benthic foraminiferal biofacies and sequence stratigraphy, Island Beach borehole, New Jersey, in: Proceedings of the Ocean Drilling Program, Scientific Results, 150X, edited by: Miller, K. G. and Snyder, S. W., Ocean Drilling Program, College Station, TX, 267–375, 1997.

Miller, K. G.: Coastal Plain Drilling And The New Jersey Sea-Level Transect, in: Proceedings of the Ocean Drilling Program, Scientific Results, Volume 150X, edited by: Miller, K. G. and Snyder, S. W., Ocean Drilling Program, College Station, TX, 3–12, 1997.

Miller, K. G., Sugarman, P. J., Browning, J. V., et al: Proceedings of the Ocean Drilling Program, Initial Reports 174AX. doi:10.2973/odp.proc.ir.174ax.1998, Ocean Drilling Program, College

A dynamic climate state during the Paleocene-Eocene Thermal Maximum

A. Sluijs and H. Brinkhuis

Full Screen / Esc

Station, TX, 1998.

Nicolo, M. J., Dickens, G. R., Hollis, C. J., and Zachos, J. C.: Multiple early Eocene hyperther-mals: Their sedimentary expression on the New Zealand continental margin and in the deep sea, Geology, 35, 699–702, 2007.

5 Pagani, M., Caldeira, K., Archer, D., and Zachos, J. C.: An Ancient Carbon Mystery, Science, 314, 1556–1557, doi:10.1126/science.1136110, 2006.

Pascher, A.: Über Flagellaten und Algen, Deutsche Botanische Gesellachaft, Berichte, 32, 136–160, 1914.

Powell, A. J., Brinkhuis, H., and Bujak, J. P.: Upper Paleocene - Lower Eocene dinoflagellate
10 cyst sequence biostratigraphy of southeast England, in: Correlation of the Early Paleogene in Northwest Europe, Geological Society Special Publication, 101, edited by: Knox, R. W. O. B., Corfield, R. M., and Dunay, R. S., 145–183, 1996.

Pross, J.: Paleo-oxygenation in Tertiary epeiric seas: Evidence from dinoflagellate cysts, Palaeogeogr. Palaeocl., 166, 369–381, 2001.

15 Pross, J. and Brinkhuis, H.: Organic-walled dinoflagellate cysts as paleoenvironmental indi-cators in the Paleogene; a synopsis of concepts, Paläontologische Zeitschrift, 79, 53–59, 2005.

Ravizza, G., Norris, R. N., Blusztajn, J., and Aubry, M.-P.: An osmium isotope excursion associ-ated with the late Paleocene thermal maximum: Evidence of intensified chemical weathering,
20 Paleoceanography, 16, 155–163, 2001.

Reichart, G.-J., Brinkhuis, H., Huiskamp, F., and Zachariasse, W. J.: Hyper-stratification follow-ing glacial overturning events in the northern Arabian Sea, Paleoceanography, 19, PA2013, doi:10.1029/2003PA000900, 2004.

Robert, C. and Kennett, J. P.: Antarctic subtropical humid episode at the Paleocene-Eocene
25 boundary: clay mineral evidence, Geology, 22, 211–214, 1994.

Rochon, A., Lewis, J., Ellegaard, M., and Harding, I. C.: The Gonyaulax spinifera (Dinophyceae) "complex": Perpetuating the paradox?, Rev. Palaeobot. Palyno., 155, 52–60, 2009

Röhl, U., Westerhold, T., Bralower, T. J., and Zachos, J. C.: On the duration of the Pale-ocene – Eocene thermal maximum (PETM), Geochemistry, Geophysics, Geosystems, 8,
30 doi:10.1029/2007GC001784, 2007.

Schmitz, B., Pujalte, V., and Nunez-Betelu, K.: Climate and sea-level perturbations during the Initial Eocene Thermal Maximum: evidence from siliciclastic units in the Basque Basin (Ermua, Zumaia and Trabakua Pass), northern Spain, Palaeogeogr. Palaeocl., 165, 299–

A dynamic climate state during the Paleocene-Eocene Thermal Maximum

A. Sluijs and H. Brinkhuis

320, 2001.

Sluijs, A., Brinkhuis, H., Stickley, C. E., Warnaar, J., Williams, G. L., and Fuller, M.: Dinoflagellate cysts from the Eocene/Oligocene transition in the Southern Ocean; results from ODP Leg 189., in: Proceedings Ocean Drilling Program, Scientific Results 189, edited by: Exon, N. F., Kennett, J. P., and Malone, M. J., College Station, Texas, 1–42, 2003.

Sluijs, A., Pross, J., and Brinkhuis, H.: From greenhouse to icehouse; organic-walled dinoflagellate cysts as paleoenvironmental indicators in the Paleogene, Earth-Sci. Rev., 68, 281–315, 2005.

Sluijs, A., Schouten, S., Pagani, M., Woltering, M., Brinkhuis, H., Sinninghe Damsté, J. S., Dickens, G. R., Huber, M., Reichart, G.-J., Stein, R., Matthiessen, J., Lourens, L. J., Pedentchouk, N., Backman, J., Moran, K., and the Expedition 302 Scientists: Subtropical Arctic Ocean temperatures during the Palaeocene/Eocene thermal maximum, Nature, 441, 610–613, 2006.

Sluijs, A., Bowen, G. J., Brinkhuis, H., Lourens, L. J., and Thomas, E.: The Palaeocene-Eocene thermal maximum super greenhouse: biotic and geochemical signatures, age models and mechanisms of global change, in: Deep time perspectives on Climate Change: Marrying the Signal from Computer Models and Biological Proxies, edited by: Williams, M., Haywood, A. M., Gregory, F. J., and Schmidt, D. N., The Micropalaeontological Society, Special Publications, The Geological Society, London, London, 323–347, 2007a.

Sluijs, A., Brinkhuis, H., Schouten, S., Bohaty, S. M., John, C. M., Zachos, J. C., Sinninghe Damsté, J. S., Crouch, E. M., and Dickens, G. R.: Environmental precursors to light carbon input at the Paleocene/Eocene boundary, Nature, 450, 1218–1221, 2007b.

Sluijs, A., Brinkhuis, H., Crouch, E. M., John, C. M., Handley, L., Munsterman, D., Bohaty, S., M., Zachos, J. C., Reichart, G.-J., Schouten, S., Pancost, R. D., Sinninghe Damsté, J. S., Welters, N. L. D., Lotter, A. F., and Dickens, G. R.: Eustatic variations during the Paleocene-Eocene greenhouse world, Paleoceanography, 23, PA4216, doi:10.1029/2008PA001615, 2008a.

Sluijs, A., Röhl, U., Schouten, S., Brumsack, H.-J., Sangiorgi, F., Sinninghe Damsté, J. S., and Brinkhuis, H.: Arctic late Paleocene–early Eocene paleoenvironments with special emphasis on the Paleocene-Eocene thermal maximum (Lomonosov Ridge, Integrated Ocean Drilling Program Expedition 302), Paleoceanography, 23, PA1S11, doi:10.1029/2007PA001495, 2008b.

Sluijs, A., Brinkhuis, H., Williams, G. L., and Fensome, R. A.: Taxonomic revision of some

A dynamic climate state during the Paleocene-Eocene Thermal Maximum

A. Sluijs and H. Brinkhuis

Cretaceous-Cenozoic spiny organic-walled, peridinioid dinoflagellate cysts, Rev. Palaeobot. Palyno., 154, 34–53 doi:10.1016/j.revpalbo.2008.1011.1006, 2009.

Sriver, R. L., and Huber, M.: Observational evidence for an ocean heat pump induced by tropical cyclones, Nature, 447, 577–580, 2007.

5 Steurbaut, E., Magioncalda, R., Dupuis, C., Van Simaeys, S., Roche, E., and Roche, M.: Palynology, paleoenvironments, and organic carbon isotope evolution in lagoonal Paleocene-Eocene boundary settings in North Belgium, in: Causes and consequences of Globally Warm Climates in the Early Paleogene, Geological Society of America Special Paper 369, edited by: Wing, S. L., Gingerich, P., Schmitz, B., and Thomas, E., Geological Society of

10 America, Boulder, Colorado, 291–317, 2003.

Taylor, F. J. R.: On dinoflagellate evolution, BioSystems, 13, 65–108, 1980.

ter Braak, C. J. F. and Smilauer, P.: CANOCO Reference Manual and User's Guide to Canoco for Windows: Software for Canonical Community Ordination (version 4.5), Microcomputer Power, Ithaca, NY, USA, 2002.

15 Wall, D., Dale, B., Lohmann, G. P., and Smith, W. K.: The environmental and climatic distribution of dinoflagellate cysts in modern marine sediments from regions in the North and South Atlantic Oceans and adjacent seas, Mar. Micropaleontology, 2, 121–200, 1977.

Wing, S. L., Harrington, G. J., Smith, F. A., Bloch, J. I., Boyer, D. M., and Freeman, K. H.: Transient Floral Change and Rapid Global Warming at the Paleocene-Eocene Boundary,

20 Science, 310, 993–996, doi:10.1126/science.1116913, 2005.

Zachos, J. C., Röhl, U., Schellenberg, S. A., Sluijs, A., Hodell, D. A., Kelly, D. C., Thomas, E., Nicolo, M., Raffi, I., Lourens, L. J., McCarren, H., and Kroon, D.: Rapid Acidification of the Ocean during the Paleocene-Eocene Thermal Maximum, Science, 308, 1611–1615, 2005.

Zachos, J. C., Schouten, S., Bohaty, S., Quattlebaum, T., Sluijs, A., Brinkhuis, H., Gibbs, S.,

25 and Bralower, T. J.: Extreme warming of mid-latitude coastal ocean during the Paleocene-Eocene Thermal Maximum: Inferences from TEX$_{86}$ and Isotope Data, Geology, 34, 737–740, 2006.

Table 1. Dinocyst events recognized at Bass River and Wilson Lake.

Event	Description	Remarks	Onset Bass River (mbs)	Termination Bass River (mbs)	Onset Wilson Lake (mbs)	Termination Wilson Lake (mbs)
A	a sharp decrease (>70% – 40%) in the abundance of *Areoligera*		362.00		112.55	
B	a short-lived acme of Goniodomid taxa		359.50	359.00	110.80	110.60
C	a second decrease in *Areoligera* abundance		358.90		110.50	
D	a short-lived abundance of *Hystrichosphaeridium*		358.00	357.40	110.50	110.00
E	the onset of the Apectodinium acme		357.70		110.40	
F	abundance of *Membranosphaera*	tentative correlation	357.60	357.30	110.30	109.90
CIE			357.35		110.00	
G	abundance of *Florentinia reichartii*	tentative correlation, not truly outstanding at Bass River	357.10		109.10	108.30
H	rapid decrease in *Apectodinium* abundance		356.90		108.00	
I	a short-lived acme of Goniodomid taxa		356.67	356.35	107.90	
J	abundance of Cordosphaeridium	tentative correlation	356.40	356.15	106.50	103.00
K	onset of abundant *Senegalinium* cpx (low salinity-tolerant)		356.25		103.80	
L	pulse in Apectodinium abundance	tentative correlation, not truly outstanding at Wilson Lake	355.60	355.10	102.70	102.60
M	second increase in *Senegalinium* cpx (low salinity-tolerant)		354.85		101.00	
N	increase in Apectodinium abundance		353.50		97.50	

A dynamic climate state during the Paleocene-Eocene Thermal Maximum

A. Sluijs and H. Brinkhuis
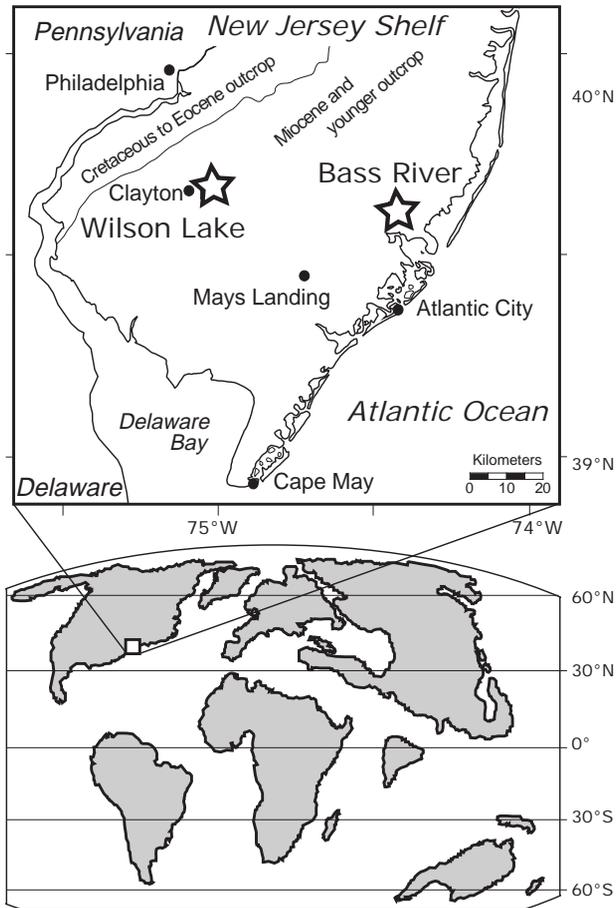
Fig. 1. Drill locations of the Wilson Lake and Bass River cores. Modified from Miller (1997).

A. Sluijs and H. Brinkhuis

Fig. 2a. Relative dinocyst distribution across the late Paleocene – Early Eocene at Bass River.

A. Sluijs and H. Brinkhuis
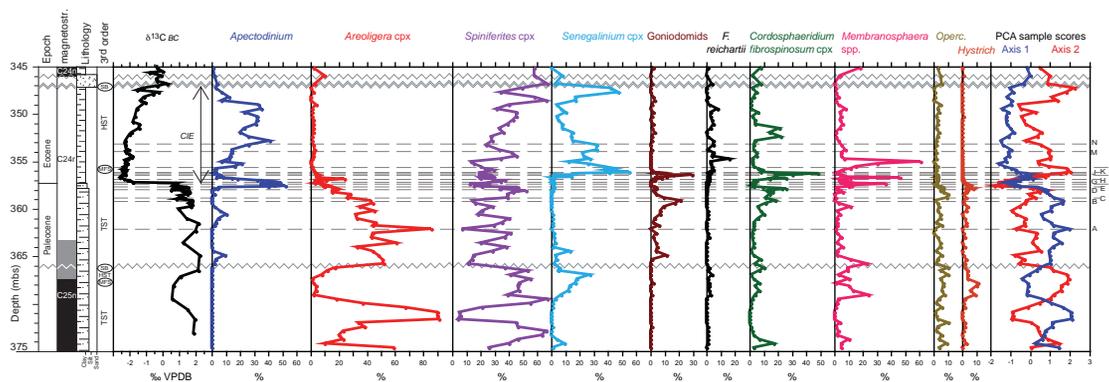
Fig. 2b. Absolute quantitative dinocyst distribution across the late Paleocene – Early Eocene at Bass River.

Title Page

Abstract | Introduction

Conclusions | References

Tables | Figures

|◄ | ►|

◄ | ►

Back | Close

Full Screen / Esc

Printer-friendly Version

Interactive Discussion

Title Page

Abstract   Introduction

Conclusions   References

Tables   Figures

◀◀   ▶▶

◀   ▶

Back   Close

Full Screen / Esc

Printer-friendly Version

Interactive Discussion

Fig. 3a. Relative dinocyst distribution across the late Paleocene – Early Eocene at Wilson Lake.

Fig. 3b. Absolute quantitative dinocyst distribution across the late Paleocene – Early Eocene at Wilson Lake.

Fig. 4. Depth-depth plot based on dinocyst events (Table 1) indicating relative sedimentation rates between Wilson Lake and Bass River.
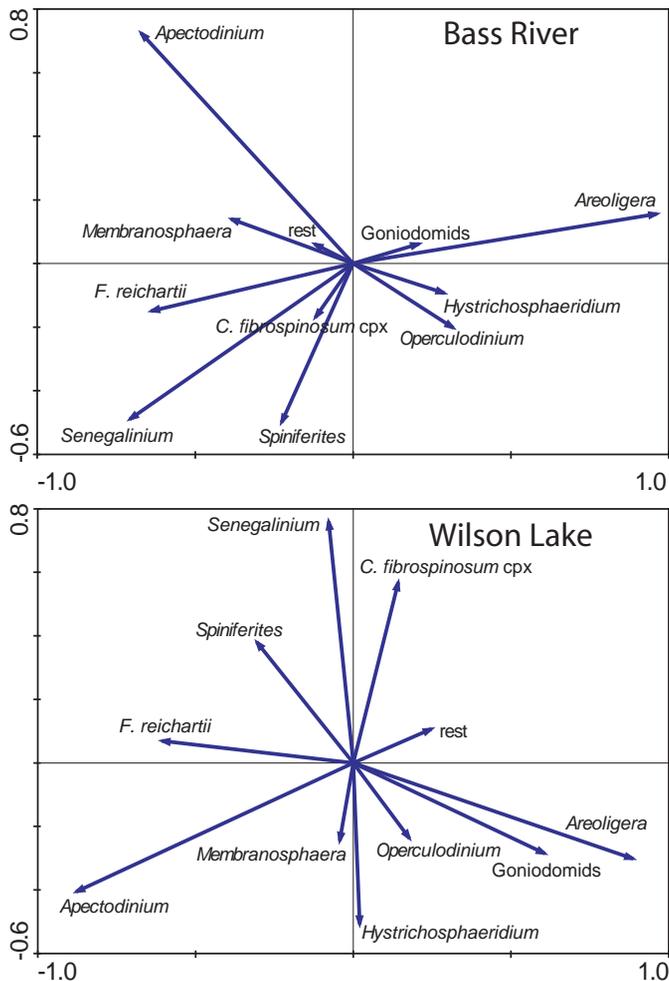
Fig. 5a. Principle Component Analysis scatter plots of Bass River and Wilson Lake.

Title Page

Abstract | Introduction

Conclusions | References

Tables | Figures

|◄ | ►|

◄ | ►

Back | Close

Full Screen / Esc

Printer-friendly Version

Interactive Discussion
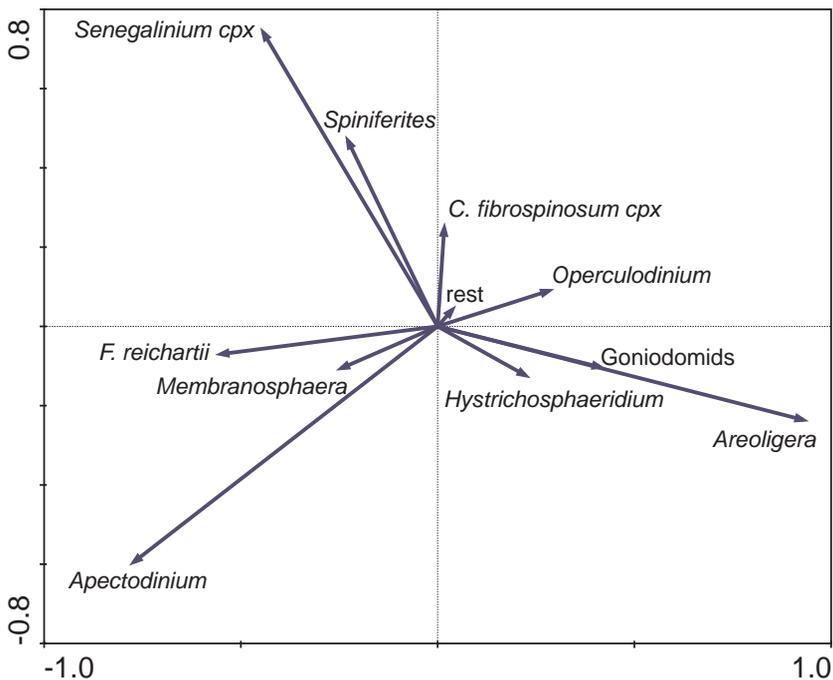
Fig. 5b. Principle Component Analysis scatter plot; combined Bass River and Wilson Lake.
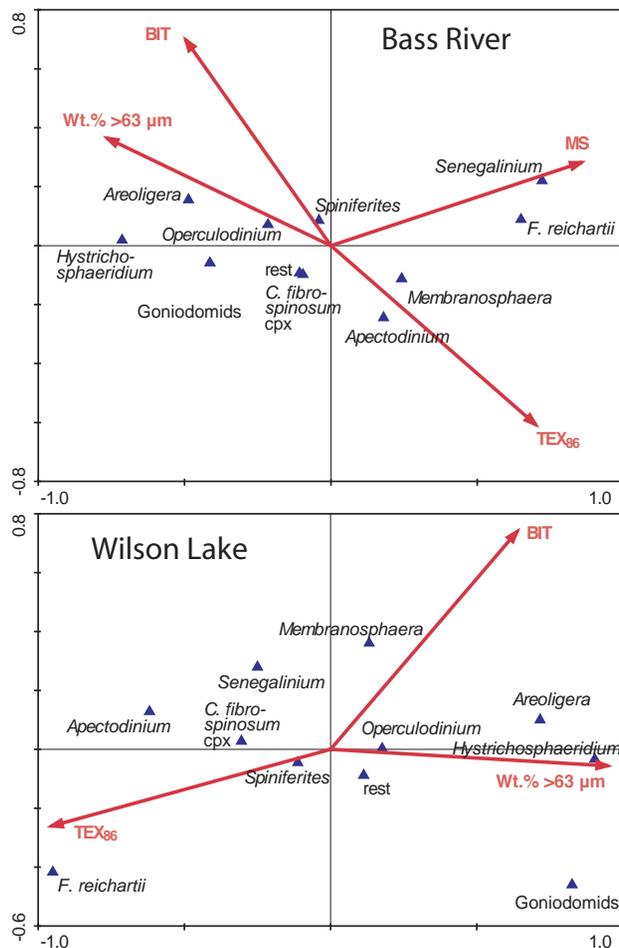
Fig. 6. Canonical Correspondence Analysis scatter plots.

Title Page

Abstract | Introduction

Conclusions | References

Tables | Figures

|◄ | ►|

◄ | ►

Back | Close

Full Screen / Esc

Printer-friendly Version

Interactive Discussion
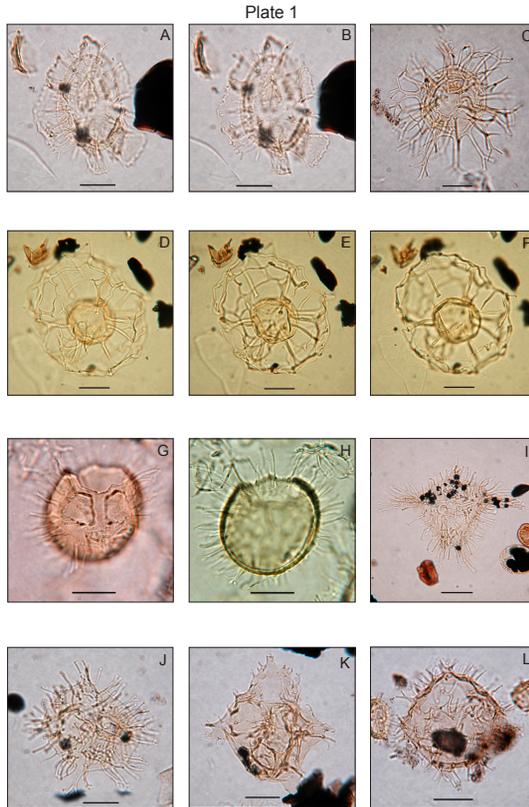
Plate 1

Plate 1. **(A–B)** *Achilleodinium biformoides* (Bass River, 357.76 mbs, #1, England Finder coordinates: M61-2); **(C)** *Achomosphaera alcicornu* (Bass River, 360.20 mbs, #1, P59-1); **(D–F)** *Adnatosphaeridium robustum* (Bass River, 358.12 mbs, #1, N56-2); **(G–H)** *Alisocysta* sp. 2 of Heilmann-Clausen (1985) (Wilson Lake, 110.0 mbs, #1, U45-1); **(I)** *Apectodinium augustum* (Wilson Lake, 107.40 mbs, #1, O59-1); **(J)** *Apectodinium homomorphum* (Bass River, 353.25 mbs, #1, L59-4); **(K)** *Apectodinium parvum* (Bass River, 354.41 mbs, #1, N63-3); **(L)** *Apectodinium quinquelatum* (Wilson Lake, 91.51 mbs, #1, M56-3). Scale bar=20 µm.
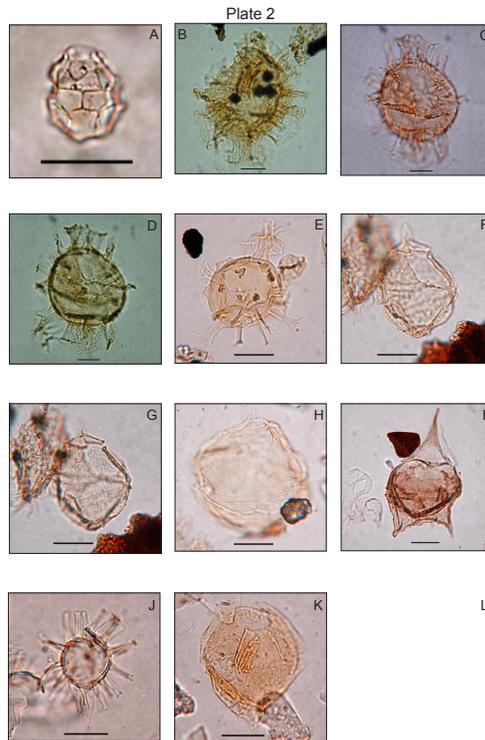
Plate 2

Plate 2. **(A)** *Cladopyxidium saeptum* (Wilson Lake, 112.76 mbs, #1, England Finder coordinates: R44-3); **(B)** *Cordosphaeridium fibrospinosum* cpx. Morphotype intermediate between *C. fibrospinosum* and *Damassadinium* spp. (Bass River, 366.20 mbs, #1, L59-3); **(C–D)** *Cordosphaeridium fibrospinosum* cpx. Morphotype intermediate between *C. fibrospinosum* and *Turbiosphaera* spp. (Bass River, 396.95 mbs, #1, M62-1); **(E)** *Cordosphaeridium fibrospinosum* (Bass River, 356.69 mbs, #1, M62-1); **(F–G)** *Cribroperidinium* spp. (Bass River, 357.30 mbs, #1, Q52-1); **(H)** *Cribroperidinium* sp. Big (Bass River, 347.13 mbs, #1, L64-2); **I** *Deflandrea oebisfeldensis* (Bass River, 374.19 mbs, #1, H55-1); **(J)** *Diphyes colligerum* (Wilson Lake, 112.76 mbs, #1, D53-3); **(K)** *Dracodinium pachyderma* (Bass River, 345.93 mbs, #1, G60-4). Scale bar=20 μm.

A dynamic climate state during the Paleocene-Eocene Thermal Maximum

A. Sluijs and H. Brinkhuis
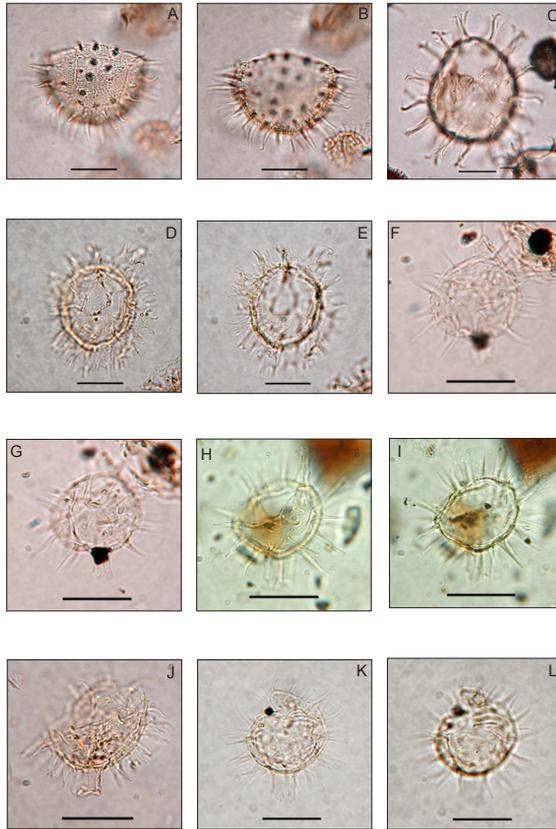
Plate 3

Plate 3. **(A–B)** *Eocladopyxis paniculatum* (Wilson Lake, 112.76 mbs, England Finder coordinates: O48-3); **(C)** *Fibrocysta* spp. (Wilson Lake, 110.14 mbs, L45-2); **(D–E)** *Florentinia ferox* (Bass River, 357.76 mbs, L62-1); **(F–L)** *Florentinia reichartii* sp. nov. ((F–G), paratype, Wilson Lake, 104.07 mbs, #1, N56-1; (H–I), paratype, Wilson Lake, 111.97 mbs, #1, O57-1; J, paratype, Bass River, 349.04 mbs, #1, L52-2; K–L, paratype, Bass River, 351.08 mbs, #1, M49-2). Scale bar=20 μm.
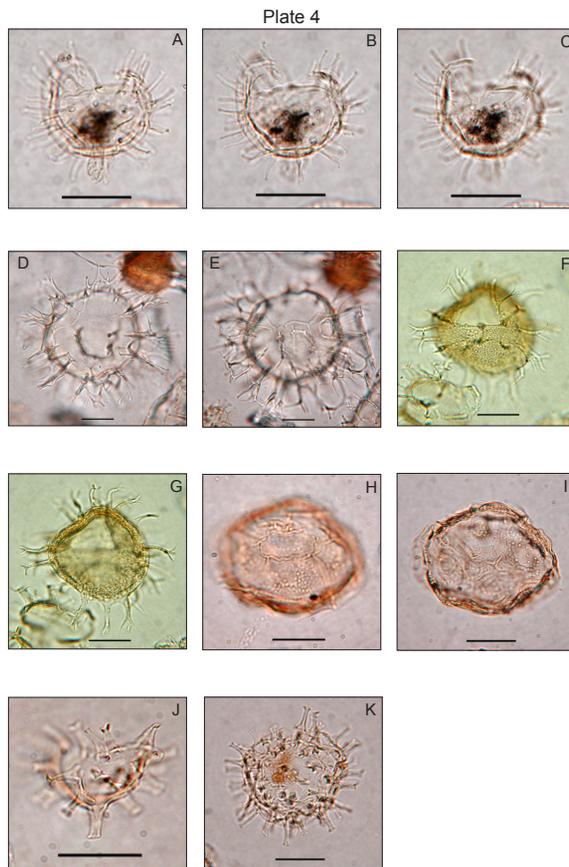
Plate 4

Plate 4. **(A–C)** *Florentinia reichartii* sp. nov. Holotype (Bass River, 355.26 mbs, #1, England Finder coordinates: N52-2); **(D–E)**, *Glaphyrocysta volata* (Wilson Lake, 112.76 mbs, #1, M49-1); **(F–G)** *Hafniasphaera septata* (Wilson Lake, 110.14 mbs, #2, L45-1); **(H–I)** *Heteraulacacysta* spp. (Wilson Lake, 110.73 mbs, #1, M56-4); **(J–K)** *Homotryblium* spp. (J, Bass River, 349.44 mbs, #1, K50-3; K, Bass River, 351.08 mbs, #1, L49-3). Scale bar=20 µm.

A dynamic climate state during the Paleocene-Eocene Thermal Maximum

A. Sluijs and H. Brinkhuis
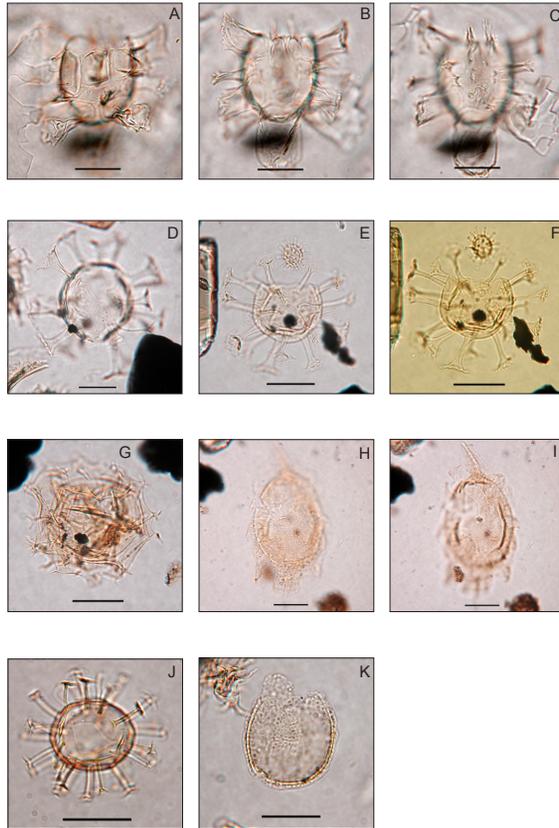
Plate 5. **(A–C)** *Hystrichokolpoma salacia* (Wilson Lake, 112.76 mbs, #1, England Finder coordinates: O48-4); **(D–F)** *Hystrichosphaeridium truswelliae* (D, Wilson Lake, 110.14, #1, G59-3; E–F, Bass River, 357.76 mbs, #1, O62-1); **(G)** *Hystrichostrogylon* spp. (Bass River, 356.69 mbs, #1, M58-1); **H–I** *Lanternosphaeridium lanosum* (Bass River, 349.44 mbs, #1, O53-3); **(J)** *Melitasphaeridium pseudorecurvatum* (Wilson Lake, 110.06 mbs, #1, N52-1), **(K)** *Membranosphaera* spp. (Wilson Lake, 110.14 mbs, J53-4). Scale bar=20 μm.
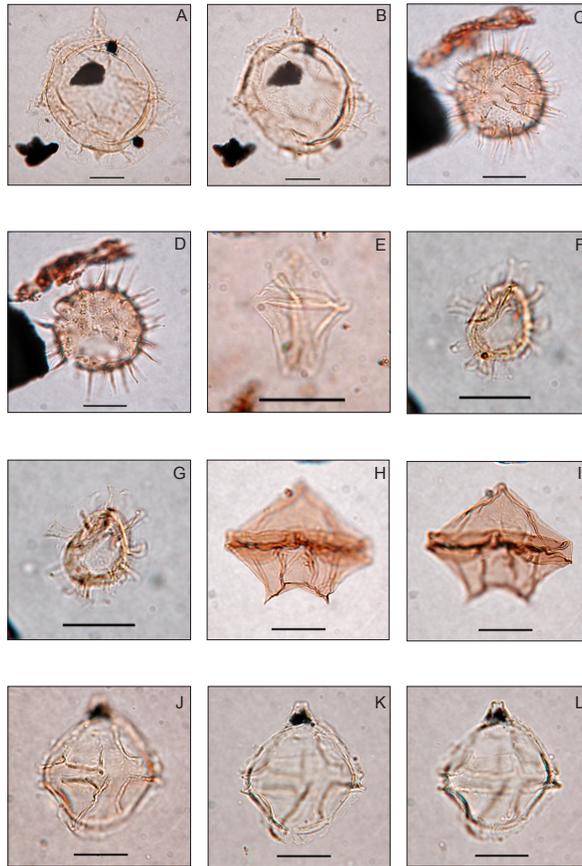
Plate 6

Plate 6. **(A–B)** *Muratodinium fimbriatum* (Bass River, 354.41 mbs, #1, England Finder coordinates: N63-3); **(C–D)** *Operculodinium* spp. (Bass River, 359.77 mbs, #1, N61-1); **(E)** *Paleotetradinium minisculum* (Wilson Lake, 111.97 mbs, #1, N52-3); **(F–G)** *Paucisphaeridium* spp. (Bass River, 357.76 mbs, L56-4); **(H–I)** *Phelodinium magnificum* (Bass River, 356.69 mbs, #1, S60-3); **(J–L)** *Phthanoperidinium crenulatum* (Wilson Lake, 95.96 mbs, #1, J44-4). Scale bar=20 μm.
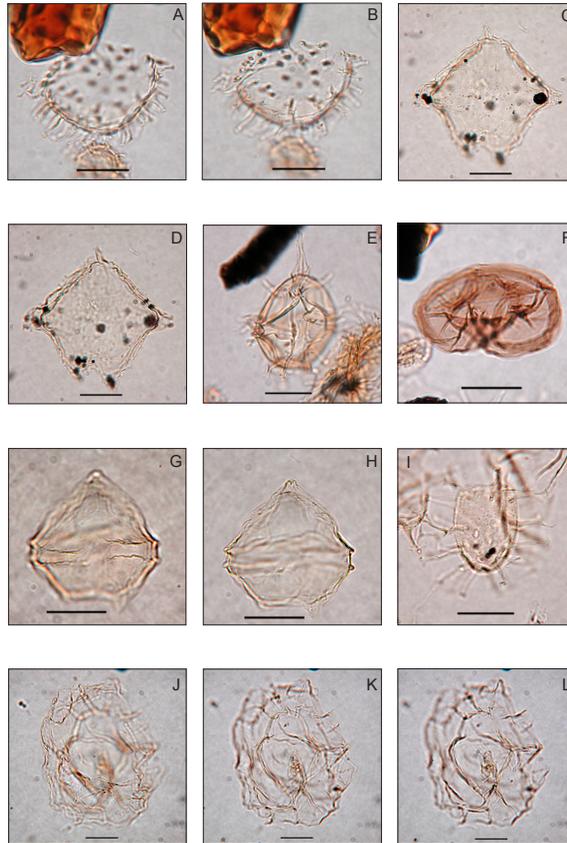
Plate 7

Plate 7. **(A–B)** *Polysphaeridium zoharii* (Bass River, 361.05 mbs, #1, England Finder coordinates: N19-1); **(C–D)** *Rhombodinium* spp. (Wilson Lake, 109.42 mbs, #1, L45-2); **(E)** *Rottnestia borrusica* (Bass River, 354.41 mbs, #1, N58-4); **(F)** *Selenopemphix nephroides* (Bass River, 356.69 mbs, #1, R61-4); **(G–H)** *Senegalinium* spp. (Wilson Lake, 94.40 mbs, #1, T57-3); **(I)** *Tanyosphaeridium* spp. (Bass River, 350.66 mbs, #1, N44-4); **J–L** *Thalassiphora delicata* (Bass River, 373.76 mbs, #1, K60-2). Scale bar=20 μm.
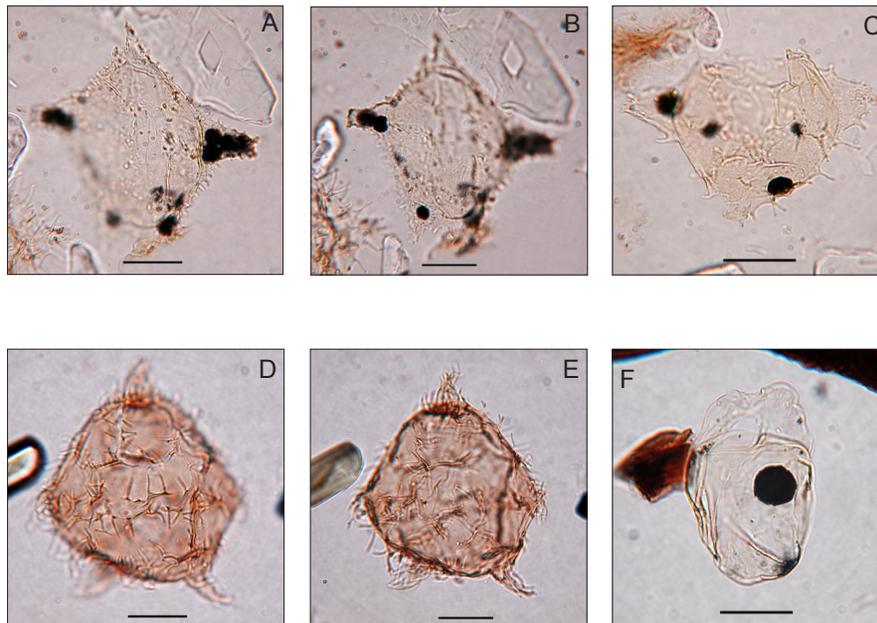
Plate 8

Plate 8. **(A–B)** *Wetzeliella articulata* (Bass River, 346. 82 mbs, #1; England Finder coordinates: N58-3); **(C)** *Wetzeliella – Dracodinium varielongitudum* (Bass River, 345.96 mbs, #1; L66-4); **(D–E)** *Wilsonidium tesselatum* (Bass River, 357.39 mbs, #1, J54-4); **(F)** *Nelsoniella* spp. (Late Cretaceous reworked; Bass River, 366.93 mbs, #1, M60-3). Scale bar=20 μm.
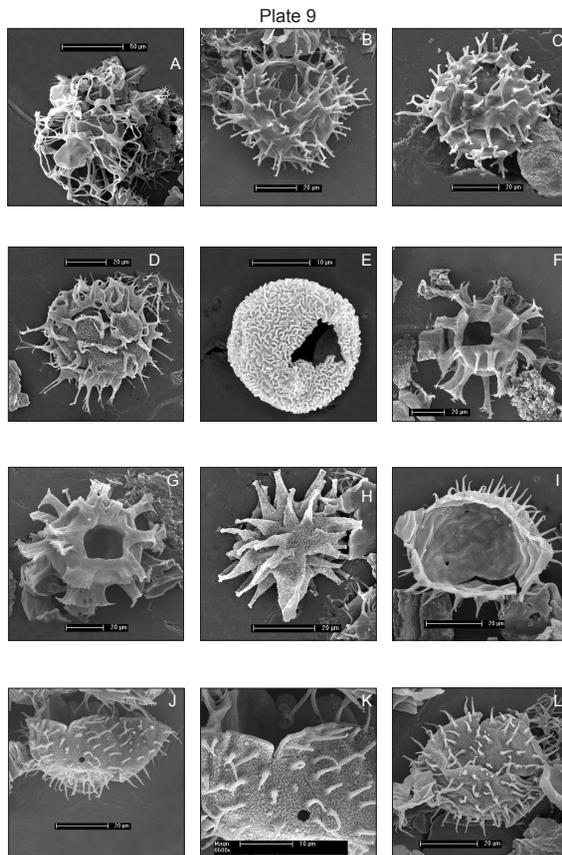
Plate 9

Plate 9. **(A)** *Adnatosphaeridium robustum* (Bass River, 364.89 mbs); **(B–C)** *Apectodinium homomorphum* (Bass River, 357.39 mbs); **(D)** *Areoligera* spp. (Bass River, 355.93 mbs); **(E)** *Cerebrocysta* spp. (Bass River, 355.93 mbs); **(F–G)**, *Cordosphaeridium fibrospinosum* (F, Bass River 356.93 mbs; G, Bass River, 355.93 mbs); **(H)** *Diphyes colligerum* (Bass River, 357.39 mbs); **(I–L)** *Eocladopyxis paniculatum* (Bass River, 364.89 mbs; K is a detail of J to indicate sutures).

A dynamic climate state during the Paleocene-Eocene Thermal Maximum

A. Sluijs and H. Brinkhuis
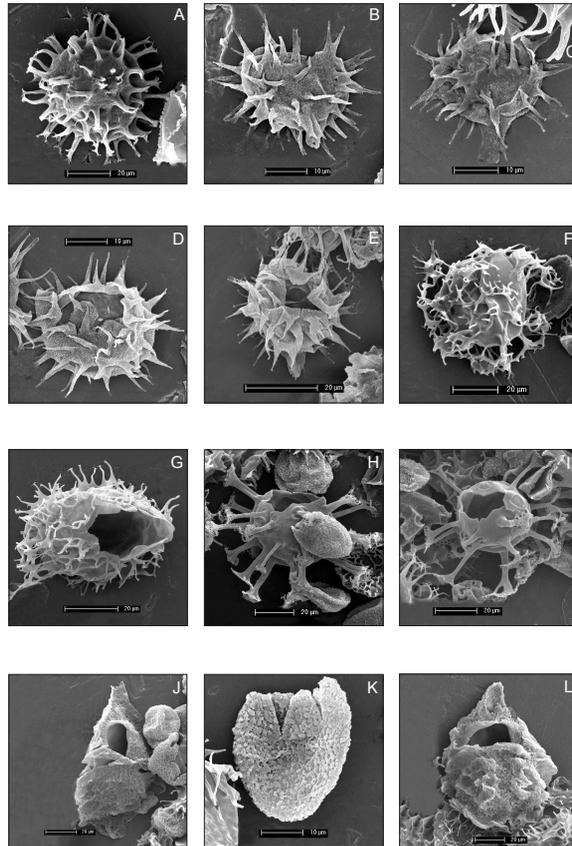
Plate 10

Plate 10. **(A)** *Fibrocysta axialis* (Bass River, 356.93 mbs); **(B–E)** *Florentinia reichartii* sp. nov. (B-D, Bass River, 356.93; E, 355.93 mbs); **(F–G)**, *Glaphyrocysta volata* (Bass River, 364.89 mbs); **(H–I)** *Hystrichosphaeridium truswelliae* (Bass River, 357.39 mbs); **(J)** *Lanternosphaeridium lanosum* (Bass River, 357.39 mbs); **(K)** *Membranosphaera* spp. (Bass River 357.39 mbs); **(L)** *Muratodinium fimbriatum* (Bass River, 357.39 mbs).

Title Page	
Abstract	Introduction
Conclusions	References
Tables	Figures
I◄	►I
◄	►
Back	Close
Full Screen / Esc	

Printer-friendly Version

Interactive Discussion

Plate 11
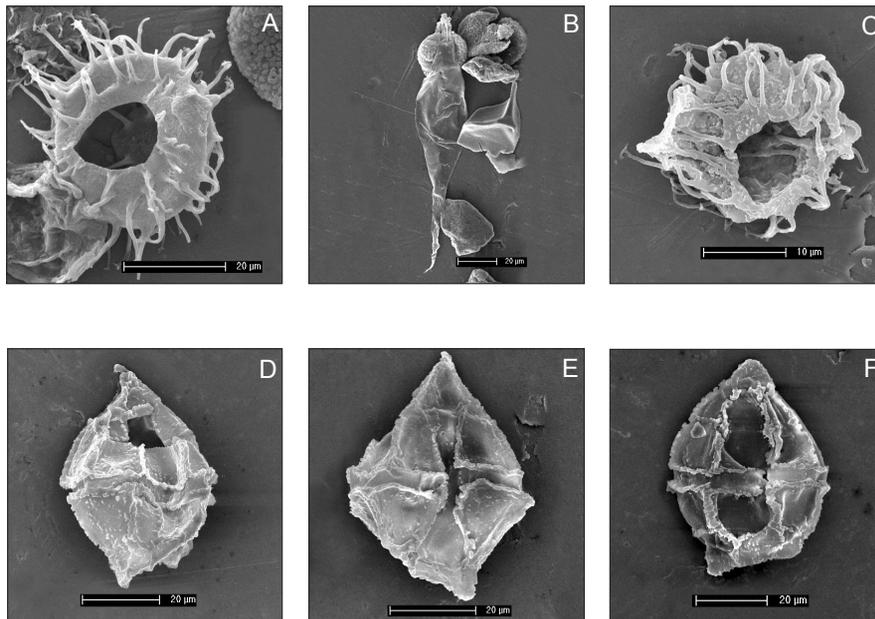
Plate 11. **(A)** *Operculodinium* spp. (Bass River, 357.39 mbs); **(B)** *Palaeocystodinium* spp. (Bass River, 357.39 mbs); **(C)** *Paucisphaeridium* spp. (Bass River 364.89 mbs); **(D–F)** *Phthanoperidinium crenulatum* (Bass River 356.93 mbs).